Understanding groundwater systems and their functioning through the study of stable water isotopes in a hard-rock aquifer (Maheshwaram watershed, India)

Philippe Négrel, Hélène Pauwels, Benoît Dewandel, Jean-Marie Gandolfi, Cédric Mascré, Mohamed-Salem Ahmed

UNDERSTANDING GROUNDWATER SYSTEMS AND THEIR FUNCTIONING THROUGH THE STUDY OF STABLE WATER ISOTOPES IN A HARD-ROCK AQUIFER (MAHESHWARAM WATERSHED, INDIA)

Ph. Negrel [α, 1], H. Pauwels[1], B. Dewandel[1, 2], J.M. Gandolfi[1, 2], C. Mascré[1, 2], S. Ahmed[2, 3]

[1] BRGM, Avenue C. Guillemin, BP 36009, 45060 Orléans Cedex 02, FRANCE.

p.negrel@brgm.fr, h.pauwels@brgm.fr, b.dewandel@brgm.fr, jm.gandolfi@brgm.fr,

[2] CEFIRES, Indo-French Center for Ground water Research, NGRI, Uppal Road, 500 007 Hyderabad, India

[3] NGRI, Uppal Road, 500 007 Hyderabad, India

shakeelahmed@ngri.res.in

Abstract

Groundwater degradation through abstraction, contamination, etc., shows a world-wide increase and has been of growing concern for the past decades. In this light, the stable isotopes of the water molecule ($\delta^{18}O$ and $\delta^{2}H$) from a hard-rock aquifer in the Maheshwaram watershed (Andhra Pradesh, India) were studied. This small watershed (53 km^2) underlain by granite, is endorheic and representative of agricultural land use in India, with more than 700 bore wells in use. In such a watershed, the effect of overpumping can be severe and the environmental effects of water abstraction and contamination are of vital importance. A detailed and dynamic understanding of groundwater sources and flow paths in this watershed thus is a major issue for both researchers and water managers, especially with regards to water quality as well as the delimitation of resources and long-term sustainability.

To this end, the input from monsoon-precipitation was monitored over two cycles, as well as measuring spatial and temporal variations in $\delta^{18}O$ and $\delta^{2}H$ in the groundwater and in precipitation. Individual recharge from the two monsoon periods was identified, leading to identification of periods during which evaporation affects groundwater quality through a higher concentration of salts and stable isotopes in the return flow. Such evaporation is further affected by land use, rice paddies having the strongest evapotranspiration.

[α] Corresponding author: p.negrel@brgm.fr; Tel.: +33 2 38 64 39 69, Fax: +33 2 38 64 34 46

Keywords: Evaporation, Groundwater, India, Monsoon, Recharge, Stable Isotopes

1. Introduction

Groundwater flow and storage in hard-rock areas are of great interest and importance to researchers and water managers (e.g., De Silva and Weatherhead, 1997; Ballukraya and Sakthivadivel, 2002), from a viewpoint of both water quantity (Gupta and Singh, 1988) and quality (Robins and Smedley, 1994), as well as for delimiting resources and aquifers (e.g., Singhal et al., 1988). In terms of hydrogeology, hard rocks are heterogeneous and anisotropic, groundwater flow generally being controlled by fissure networks (Maréchal et al., 2004).

Typically, hard-rock aquifers occupy the first tens of metres below ground (Detay et al., 1989). Their hydrodynamic properties derive primarily from weathering processes (Wyns et al., 1999; Taylor and Howard, 2000; Dewandel et al., 2006), where hostrock minerals are transformed into mainly clay-rich materials at surface equilibrium (Tardy, 1971; Nahon, 1991). From the top downward, hard-rock aquifers consist of two main layers: saprolite or regolith—a clay-rich material derived from prolonged in-situ weathering of the hostrock—and a fissured layer characterized by dense sub-horizontal and -vertical fracturing in the first metres, below which fissure density decreases with depth (e.g. Dewandel et al., 2006). Such fractures either pre-existed or were caused by the swelling of certain minerals (e.g. biotite in granite), resulting in a local volume increase that generates cracks and fracturing. The fresh basement below is only locally permeable, where tectonic joints and fractures are present.

In India, as in other rapidly developing countries, groundwater use for domestic, industrial and agricultural activities is growing fast. Groundwater now irrigates 27 million hectares of farmland in India, a larger area than that irrigated by surface water (21 million ha). This change in water use has been extremely rapid since the start of the ‘Green Revolution’ in the 1970s; the number of bore wells has also increased enormously in the past 40 years, from less than one million in 1960 to over 26 million in 2007. For that reason, groundwater

resources are under great stress, especially in hard-rock and (semi)arid areas, due to the abstraction of large quantities of water through pumping for irrigation that undermines the sustainability of water availability and agricultural development. Over the last decade, much of India, and particularly Andhra Pradesh, Karnataka, Maharasthra, Madhya Pradesh and Rajasthan, has suffered from drought, severe drops in groundwater level, and an alarming deterioration of water quality. It is thus imperative that groundwater resources be carefully managed and that institutions in charge of water management be equipped with suitable tools (Dewandel et al., 2007b).

Sustainable use of groundwater is quantitatively related to such factors as the volume of the existing resource, recharge, and associated environmental factors. From a groundwater-quality viewpoint, sustainability implies the prevention of deterioration of groundwater quality beyond acceptable and well-defined limits.

Stable isotopes of the water molecule have been investigated throughout India, as a support of fluoride-release investigations (Tirumalesh et al., 2007), as a tool for recharge and water-pathway characterization (Gupta et al., 2005; Sukhija et al., 2005; Mukherjee et al., 2007), for geothermal-water investigations (Majumdar et al., 2005), and for isotopic fingerprinting of paleo-climates in groundwater (Kulkarni et al., 1995; Sukhija et al., 1998). However, the trend of increasing groundwater exploitation has induced a major use of isotope tracing over the past three decades (Kumar et al., 1982; Gupta and Deshpande, 2005; Mukherjee et al., 2007; Négrel et al., 2007; Murad and Krishnamurthy, 2008). The main contribution of stable isotopes in fractured-rock hydrogeology concerns the identification of variably mixed groundwater reservoirs, of groundwater flow, and of resource renewal (Fontes, 1980, Praamsma et al., 2009).

The Maheshwaram watershed is representative of watersheds in southern India in terms of geology, overpumping of its hard-rock aquifer (more than 700 classical open-end

84 wells in use), its cropping pattern (rice dominating), and its rural socio-economy mainly based
85 on traditional agriculture (Dewandel et al., 2007a). Groundwater resources face chronic
86 depletion, reflected in a strongly declining water table induced by a negative groundwater
87 balance (Maréchal et al., 2006).

88 The aim of this work, based on a detailed study of the isotopic composition of
89 groundwater and rainfall in the Maheshwaram watershed (Négrel et al., 2007), was to
90 investigate the use of stable isotopes of the water molecule for tracing and fingerprinting the
91 processes of groundwater-recharge (e.g. the monsoon input) and water-use in this typical rural
92 Indian watershed experiencing agricultural water-resource overexploitation. As return flow
93 was suspected to be an important process, a major goal of this investigation was to determine
94 its potential impact on groundwater.

95 2. General features of the catchment

96 The 53 km^2 Maheshwaram watershed (Fig. 1) is located 35 km south of Hyderabad (Ranga
97 Reddy District, State of Andhra Pradesh). The area has a relatively flat topography with
98 elevations between 590 and 670 m above sea level and no perennial streams (Kumar and
99 Ahmed, 2003).

100 The semi-arid climate is controlled by the periodicity of the monsoon (rainy season:
101 June–October). Mean annual precipitation is around 750 mm, more than 90% of which falls
102 during the monsoon season. The mean annual temperature is about 26 °C, but during summer,
103 from March to May, maximum temperatures can reach 45 °C. The ratio of potential
104 evaporation from soil plus transpiration by plants (1800 mm/year) against the total quantity of
105 rainwater, yields an aridity index of 0.42, typical of semi-arid areas (Maréchal et al., 2006).
106 Surface streams are dry most of the year, except for a few days after very heavy rainfall
107 during the monsoon.

The area is underlain by Archean granite (Fig. 1; Dewandel et al., 2006). The rock is mainly orthogneissic granite with porphyritic K-feldspar. Intrusive leucocratic granite with a lower biotite content forms small hills and boulder-strewn outcrops. The weathering profile of these granites generally shows a thin layer of red soil (10–40 cm), a 1 to 3 m thick layer of sandy regolith, a 10 to 15 m thick layer of laminated saprolite, fractured granite that occupies the next 15 to 20 m and, farther down, fresh granite.

The groundwater budget of the depleted unconfined aquifer in the watershed can be summarized as follows. Horizontal groundwater inflow and outflow of the aquifer are very low compared to other terms (about 1 mm/year) and their difference is close to nil (Maréchal et al., 2006), baseflow representing groundwater discharge to streams or springs being nil (Kumar and Ahmed, 2003; Maréchal et al., 2006). Groundwater recharge is mainly direct as no permanent or temporary streams exist and only two tanks can serve as a source of indirect recharge (Dewandel et al., 2007b). The irrigation-return flow, according to Dewandel et al. (2007a), is variable in the area as a function of land-use (higher in rice paddies than in flower or vegetable plots) and evaporation from the water table is quasi nil (Maréchal et al., 2006). The water table for June 2002 (Maréchal et al., 2006) roughly follows the topographic slope, as is common in flat hard-rock areas. Water-table levels fluctuate between 610 and 619 masl, compared to a flat topography with elevations of 670 to 690 m. The water table is thus everywhere in the fissured aquifer layer, but local cones of depression occur in areas where groundwater abstraction is high due to strong pumping for irrigation.

3. Sampling procedures and analytical methods

About 700 open-end wells fitted with submersible pumps, with depths ranging from 30 to 60 m, are used for irrigation in the Maheshwaram watershed (Maréchal et al., 2006). The water samples were collected from these operational agricultural wells. Water temperature,

electrical conductivity (EC) and pH of each sample were measured *in situ*, EC with a conductivity meter standardized to 20 °C and pH using a pH electrode previously calibrated with standard buffers. Samples for stable-isotope determinations were stored in 50 ml high-density polyethylene bottles with small necks and caps sealed with paraffin film. The stable isotopes ^{2}H and ^{18}O were measured using a Finnigan MAT 252 mass spectrometer with a precision of 0.1‰ *vs.* SMOW (Standard Mean Ocean Water) for $\delta^{18}O$ and of 0.8‰ for $\delta^{2}H$. Isotopic compositions are plotted in the usual δ-scale in ‰ with reference to V-SMOW (Vienna Standard Mean Ocean Water) according to δ_{sample} (‰) = {(R_{sample} / $R_{standard}$) - 1}* 1000, where R is the $^{2}H/^{1}H$ or $^{18}O/^{16}O$ atomic ratio. Chloride analyses were performed by ion chromatography (uncertainty of 10% with a coverage factor k = 2), after filtration through 0.45 mm acetate filters (Pauwels et al., 2007).

In January 2006, after the rainy period, we selected a network of 24 open-end wells from the over 700 existing ones in the watershed for the groundwater collection to be representative of watershed recharge. In March 2006, the same network of open-end wells was sampled plus two others. One of the rare surface waters, a tank fed by the monsoon rains and afterwards only affected by evaporation, was also sampled several times to be representative of evaporation. Further sampling concerned 23 of the open-end wells from the network in July 2006, 11 open-end wells in November 2006, and 9 open-end wells in June 2008 and February 2009. During the different collection surveys, groundwater temperatures were 25.9 to 30.1 °C.

In addition to the groundwater surveys, monsoon rainfall was collected for isotope characterization of the rainwater input into the watershed. To this end, rainfall gauge RF (Fig. 1) was designed and installed in the meteorological station of Maheshwaram village. As the samples were collected on a monthly basis, the isotopic composition of the sample was likely to be modified by evaporation. This was minimized by a special construction of the rain

157 gauge, which included a 1.2-m-deep concrete excavation with a water depth of around 30 cm,
158 in which a cool box was placed. A 15-cm-diameter tube connected the 5-litre collection bottle
159 to the rain-gauge funnel. A lid for lowering the evaporation and preserving the collecting
160 system from direct input of the monsoon sealed the excavation.

161 During this study, we tried to reproduce the effect of evaporation on the basis of pan
162 evaporation (Jhajharia et al., 2009). Evaporated water samples were taken from a galvanized
163 evaporation pan installed far from vegetation and about 10 cm above the ground. The
164 operating water level in the pan at the start of the experiment was 270 mm and the volume
165 was 109.9 L from the rim. The experiment covered 55 days between November 2 and
166 December 27, 2007, and concerned the analysis of Cl^- contents and the stable isotopes δ^2H
167 and $\delta^{18}O$, as described by Kattan (2008) from Syria.

168 # 4. Results

169 ## 4.1. δ^2H AND $\delta^{18}O$ ISOTOPIC SIGNATURES OF THE MONSOON

170 The collection station in Maheshwaram village was operational from June to November 2006
171 and six monthly samples were collected. The results are given in Table 1. The amount of
172 water ranged from 0.25 L in November to 4 L in September 2006. In all, 11 L of rainwater
173 were collected for 10.5 L recorded by the meteorological station. Moreover, the linear
174 relationship (R squared = 0.996) observed for the individual points (Iso_Rainfall gauge = 1.05
175 x Meteo_Rainfall gauge + 0.02; n = 7) confirms that all the monsoon rainfall was collected
176 for the isotope survey (Table 1). The 2006 monsoon gave 517 mm of precipitation input on
177 the watershed, which is considered as a low monsoon. The isotopes in the precipitation varied
178 between -1.2‰ in June and -6.9‰ in October for $\delta^{18}O$, and between 0.2‰ and -44.4‰ for
179 δ^2H. The mean weighted isotope compositions for the precipitation are -3.83‰ and -21.69‰
180 for $\delta^{18}O$ and δ^2H, respectively (Table 1). These values are less depleted than those recorded at

181 the nearby Hyderabad station with a mean weighted $\delta^{18}O$ between April and November 1998
182 of -6.5‰ (Sukhija et al., 2006), or than those from the Lower Maner Basin (Andhra Pradesh,
183 north of Maheshwaram) where monthly composite precipitation samples in 1977 gave ranges
184 of -4.1 up to -5.1‰ for $\delta^{18}O$ and of -25.7 up to -33.4 for $\delta^{2}H$ (Kumar et al., 1982).

185 During the main rainy season (June to September), the west coast of India receives
186 influx from the Arabian Sea as the monsoon blows in from the southwest and is uplifted by
187 the Western Ghats. This section of the southwest monsoon is called the "Arabian Sea branch"
188 (hereafter referred to as SW monsoon), generally with a low depletion of heavy isotopes
189 (Deshpande et al., 2003; Gupta et al., 2005). In the Bay of Bengal, the monsoon current then
190 takes a south-easterly turn, entering the Indo-Gangetic plains after being replenished with
191 moisture from the Bay of Bengal. This section of the Indian monsoon is called the "Bay of
192 Bengal branch" (hereafter referred to as NE monsoon) generally yielding a much larger
193 depletion of heavy isotopes (Deshpande et al., 2003; Gupta et al., 2005).

194 In Maheshwaram, almost 70% of the rainfall is contributed by the SW monsoon from
195 June to September and the rest by the NE monsoon from October to November (Kumar and
196 Ahmed, 2003). During the 2006 monsoon this was quite different, with 54% of the rain falling
197 from June to August and 46% from September to November. This indicates a change in the
198 distribution between the two monsoons, as has been observed regularly since the 1990s with
199 mean values of 59% and 41%, respectively, for the SW and NE monsoons (data are from the
200 meteorological station in Maheswharam). During the collection period, the $\delta^{18}O$ and $\delta^{2}H$ fell
201 in two groups as illustrated on Figure 2. The first group yielded slightly depleted values of -
202 1.2 to -2.6‰ ($\delta^{18}O$) and 0.2 to -11.4‰ ($\delta^{2}H$) that represent the SW-monsoon input between
203 June and August, while the second one, between September and November, yielded a much
204 larger depletion of heavy isotopes with values of -5.5 to -6.9‰ ($\delta^{18}O$) and -34.4 to -44.4‰
205 ($\delta^{2}H$), a typical range for the NE monsoon. Considering the distribution of the two monsoons,

206 the SW monsoon became less and less dominant and thus the mean value of the rainfall was
207 less and less depleted for $\delta^{18}O$ (around -3.83‰ for this study), compared to the previously
208 reported values of less than -5‰ for $\delta^{18}O$ (Kumar et al., 1982; Sukhija et al., 2006).

209 Overall, when compared to the values from the SW and NE monsoons, the mean
210 weighted values are depleted for the NE monsoon (-43.1 and -6.43‰ for $\delta^{2}H$ and $\delta^{18}O$,
211 respectively) while they are enriched for the SW one (-3.5 and -1.6‰ for $\delta^{2}H$ and $\delta^{18}O$,
212 respectively), which agrees with previous studies (Deshpande et al., 2003; Gupta et al., 2005).
213 The NE monsoon was found to have values of around -60.7 and -8.8‰ for $\delta^{2}H$ and $\delta^{18}O$,
214 while the SW monsoon gave -17.1 and -3.0‰ for $\delta^{2}H$ and $\delta^{18}O$.

215 We reproduced the monsoon collection in 2008 from June to November with a further
216 six monthly samples. Similar to the 2006 monsoon, 12 L of rainwater was collected giving
217 620 mm of precipitation input on the Maheshwaram watershed. The isotopes in the 2008
218 precipitation varied in the same range as those of the 2006 monsoon (Table 1), with $\delta^{18}O$
219 ranging from 0.1‰ to -7.4‰ and $\delta^{2}H$ from 5.6‰ to -49.7‰. The mean weighted isotope
220 compositions for the precipitation are -3.39‰ and -17.05‰ for $\delta^{18}O$ and $\delta^{2}H$, respectively
221 (Table 1). As illustrated on Figure 2, the two mean values are very close. As for the 2006
222 monsoon (Fig. 1), the two monsoon branches can be seen on Figure 2.

223 The rainwater-isotope data collected at the Maheshwaram station define a linear
224 relationship $\delta^{2}H = 7.64\pm0.26 \times \delta^{18}O + 7.80\pm1.18$ ($R^2 = 0.989$, n = 12). We used FREML
225 (Functional Relationship Estimation by Maximum Likelihood, AMC, 2002) to give the best
226 estimate of the slope and intercept of the co-variation. This local meteoric water line falls
227 between the global meteoric water line $\delta^{2}H = 8\delta^{18}O + 10$ of Craig (1961) and the linear
228 relationship $\delta^{2}H = 7.6\delta^{18}O + 6.3$ given by Kumar et al. (1982). The 1997 and 1998 monsoon
229 data from the *Global Network of Isotopes in Precipitation* (IAEA/GNIP database on the web:

http://isohis.iaea.org), the data of which define a linear relationship given as $\delta^2H = 6.91 \times \delta^{18}O + 2.50$ ($R^2 = 0.989$, n = 12), differ from those obtained during this study.

4.2. δ^2H AND $\delta^{18}O$ ISOTOPIC SIGNATURES OF GROUNDWATER

Results of isotopic analyses for the groundwater collected at different periods are given in Table 2. The isotope composition in the open-end well network shows a wide range in isotope compositions from -0.6 to -4.1‰ for $\delta^{18}O$ and from -6.6 to -33.1‰ for δ^2H.

The main causes of variations in the stable-isotope signature of groundwater are natural variations in the isotopic composition of rainfall, mixing with pre-existing waters, and evaporation during percolation through soil and/or the unsaturated zone (Kendall and McDonnell, 1998). In view of the temperatures generally encountered in the subsurface, the stable isotopes of water can be considered as conservative and not affected by exchanges with soil or rock (Barth, 2000).

The δ^2H and $\delta^{18}O$ values of the groundwater samples collected in January are plotted on Figure 2 with the local meteoric water line and its 95% uncertainty envelopes (LMWL), and the global meteoric water line (GMWL, Craig, 1961); those earlier defined by Kumar et al. (1982) plot in the 95% LMWL uncertainty envelopes and are not shown on the figure. Figure 2 shows only the data obtained in January, which represent recharge that mixed with pre-existing water. Figure 2 also shows all sampling periods (January plus March, July and November 2006, June 2008 and February 2009). Groundwater in the watershed collected in January 2006 defines a co-variation with a statistically significant correlation when tested with Pearson's parametric or Spearman's nonparametric tests for correlation with values of 0.985 (at $\alpha = 0.05$). Using FREML, the equation is $\delta^2H = 6.17 \pm 0.25 \times \delta^{18}O - 0.54 \pm 0.67$ (n = 24). Groundwater also defines a co-variation in March, June, November 2006, June 2008 and February 2009 with Pearson and Spearman's R coefficients higher than 0.98. The equations

255 are given in Table 3 for all periods and few differences can be observed considering the 95%
256 uncertainty envelopes.
257
258 4.3. IMPACT OF EVAPORATION ON δ^2H AND $\delta^{18}O$ ISOTOPIC SIGNATURES
259 The δ^2H–$\delta^{18}O$ relationship due to evaporation of water can be predicted on the basis of a
260 steady-state isotope-balance model using temperature, humidity, isotopes in precipitation and
261 a liquid-vapour equilibrium model. This is based on the Craig-Gordon model (see review in
262 Gat, 2008). A slope of around 4 in a δ^2H–$\delta^{18}O$ relationship is generally observed either in
263 surface water during dry-season flow (Négrel and Lachassagne, 2000; Gibson et al., 2008), or
264 in the prediction of the Craig-Gordon model for an open-water dominated evaporative system.
265 Allison et al. (1984) showed a slope of between 4 and 6 in a δ^2H–$\delta^{18}O$ relationship for the
266 residual liquid when water evaporates from lakes and rivers or saturated soil, and of between
267 2 and 5 when evaporation affects an unsaturated soil profile.
268 A pan evaporation experiment was carried out for 55 days between 2 November and
269 27 December 2007. Starting with a Cl^- of 4.2 mg L^{-1}, it reached 33 mg L^{-1} at the end of the
270 experiment, leading to a concentration factor of 7.9. At the same time, the water volume
271 decreased from 109.9 L at the start to reach 20.6 L at the end, i.e. a factor of 5.3. The δ^2H and
272 $\delta^{18}O$ started with respective values of -15.11 and -1.58‰ and reached respectively +65.06 and
273 +17.73‰ 55 days later; this corresponds to the equation
274 $\delta^2H = 4.19 \pm 0.09 \times \delta^{18}O - 9.17 \pm 0.98$ (using FREML, $R^2 = 0.998$, n = 5)
275 reflecting an evaporation relationship with a slope of 4.19±0.09 (Fig. 3a). This value fully
276 agrees with the evaporation slopes of about 4.7 given by Navada et al. (1999) for Rajasthan
277 and of around 4.9 found by Kulkarni et al. (1995) in the central Indo-Gangetic plain.
278 One of the rare surface waters, a tank in the centre of the watershed, was sampled in
279 March and September 2006 and in February 2009 to be representative of evaporation, as the

tank was fed by monsoon rain and afterwards was only affected by evaporation. The δ^2H and $\delta^{18}O$ values of the tank water plot along the line defined by the pan-evaporation experiment, corroborating the effect of evaporation on this surface water (Fig. 3a).

Deuterium excess ('D-excess') in groundwater samples is expressed as $\delta D - 8\delta^{18}O$. The 'D-excess' values are <10, ranging from 1.1 to 7.5 in January, from -0.6 to 7.6 in March, from -9 to 7.5 in June, from -5.7 to 7.3 in November 2006, and from -4.5 to 7.2 in June 2008. The tank sample shows a 'D-excess' of -7.9 in March, -2.2 in November and -28.2 in February 2009. The lowest 'D-excess' values in the open-end wells are always observed for the M35 (around -9). The 'D-excess' values are plotted versus $\delta^{18}O$ on Figure 4.

The water loss through evaporation in semi-arid zones is illustrated on Figure 3b where $\delta^{18}O$ values for the pan experiment and the tank are plotted versus Cl contents. Starting from the mean monsoon (2006 and 2008), dissolved salts in the evaporation experiment concentrate by evaporation steps and the $\delta^{18}O$–δ^2H values have a slope reflecting kinetic fractionation; the Cl^-–$\delta^{18}O$ relationship should thus be positively correlated as any increase in evaporation would result in isotopic enrichment as well as in a higher Cl content. The Cl–$\delta^{18}O$ relationship defines a steep slope as less isotope variations would occur with increasing salinity (Fig. 3b). Compared to this natural evolution, the tank also integrates the input of Cl through human and agricultural activities, causing an increase in Cl content that can be quite large, as shown by the February 2006 sample.

5. Discussion

5.1. DISTRIBUTION OF RECHARGE IN SPACE

The δ^2H and $\delta^{18}O$ values of the groundwater samples collected in January 2006 lie closely around the local meteoric water line (LMWL, Fig. 2), confirming that the groundwater most

probably comes from present-day precipitation, though with a significant shift to the right of the LMWL. This reflects only evaporation during the percolation through soil and saprolite, as evaporation from the water table is nil (Maréchal et al., 2006) although an enrichment in heavy isotopes by irrigation-return flow is possible as well. Percolation through soil and saprolite may generate the shift to the right of the LMWL; Lee et al. (2007) showed that soil waters in a $\delta^{18}O$–$\delta^{2}H$ space plot close to the local meteoric water lines, indicating recharge from year-round precipitation and negligible evaporation, even during the hot summer season. Mathieu and Bariac (1996), studying groundwater recharge, found fast and direct infiltration through conducting fissured zones, generating $\delta^{18}O$ values at a depth of a few metres that were close to the mean rainfall input, while slow infiltration through soil and the upper 0.5 m of weathered basement rock generated enriched $\delta^{18}O$ values. Sami (1992), in South Africa, also found some evaporative enrichment in groundwater during recharge, as did Navada et al. (1999) and Nair et al. (2001) in Rajasthan who showed a similar $\delta^{2}H$–$\delta^{18}O$ relationship in groundwater as we did, and also found similar $\delta^{18}O$ values at depth (>10m) as well as enriched values in the first metre of soil and saprolite.

The $\delta^{2}H$– $\delta^{18}O$ relationship (Fig. 2) intercepts the LMWL around $\delta^{18}O = -5.5‰$, suggesting this value to be the approximate $\delta^{18}O$ composition of rainwater. However, this value of -5.5‰ disagrees with the weighted mean monsoon value of -3.39 to -3.83‰ determined in this study, and also disagrees with that of Kumar et al. (1982) who gave a $\delta^{18}O$ ranging from -4.1 to -5.1‰. Moreover, the distribution of groundwater values on Figure 2 shows some points that plot around the LMWL close to the mean monsoon value. Evaporation of representative water of the mean monsoon value alone cannot be the process that causes a shift from the LMWL, considering the mean $\delta^{18}O$ composition of the monsoon (-3.39 to -3.83‰) and the pan-evaporation experiment that led to a slope of 4.19±0.09, quite different from the groundwater one (6.17±0.25). This suggests different stages of groundwater

329 recharge with isotope signatures in close connection with those of the dual monsoon as shown
330 also by Deshpande et al. (2003) for shallow groundwater in southern India. Thus, the first step
331 is related to input from the SW monsoon, resulting in slightly depleted $\delta^{18}O$ values, while the
332 second one is related to input from the NE monsoon yielding much more depleted $\delta^{18}O$
333 values. The linear relationship defined in the groundwater thus reflects the mixing between
334 the two rainfall inputs, explaining the data distribution along the $\delta^{18}O$ line ranging from -5‰
335 to -0.5‰. Some groundwater clearly reflects a recharge due to the SW monsoon without any
336 significant influence of the NE one, which may reflect a saturated soil that limited rainwater
337 percolation during the second monsoon stage. On the contrary, the few points that are more
338 depleted when compared to mean monsoon values are more influenced by the NE monsoon.
339 The 6.17±0.25 slope of the linear relationship between all points in the $\delta^{2}H$– $\delta^{18}O$ plot,
340 differs from that of LMWL (7.64±0.26) and is caused by a larger influence of evaporation
341 affecting groundwater recharge during the SW monsoon. The water loss through evaporation
342 in semi-arid areas assumes importance as the heavy-isotope content of groundwater becomes
343 enriched relative to that of precipitation (Fontes, 1980; Navada et al., 1999; Nair et al., 2001;
344 Kattan, 2008). This suggests that the transfer velocity from rainfall towards groundwater
345 storage through soil and the unsaturated zone is sufficiently low, and that post-precipitation
346 evaporation during the passage in soil and the unsaturated zone is an active process, having a
347 greater impact for the second part of the monsoon period than for the first part, as also
348 suggested by Navada et al. (1999) in Rajasthan, Majumdar et al. (2005) in eastern India, and
349 Gupta et al. (2005) in central India. However, this is contrary to the observations by Stüber et
350 al. (2003) in West Bengal and by Négrel et al. (2007) on the Subarnarekha River system
351 (Jharkhand State).
352 This is further shown by the plot of 'D-excess' *vs.* $\delta^{18}O$ (Fig. 4). The 'D-excess'
353 values in groundwater samples are less than 10 (range -0.6 to 7.6) and fluctuate together with

354 the $\delta^{18}O$ (Pearson and Spearman's R coefficients of around -0.85). Therefore, 'D-excess'
355 values of around 8 in groundwater may be inherited from precipitation during the monsoon as
356 their similarity with the $\delta^{18}O$ monsoon values confirms minor evaporation (Deshpande et al.,
357 2003; Gupta et al., 2005). 'D-excess' values of less than 5, however, suggest significant
358 evaporation of rainwater, leaving the residual groundwater with lower 'D-excess' values and
359 depleted $\delta^{18}O$. The water in the tank plots along the same relationship, with 'D-excess' values
360 close to the lowermost ones observed in groundwater (Fig. 4). This confirms that evaporation
361 has a similar impact on ground- and surface waters.
362
363 5.2. EVOLUTION OVER TIME OF STABLE ISOTOPES IN GROUNDWATER
364 *5.2.1. Water dynamics at the watershed scale*
365 Groundwater in the watershed is defined by co-variations in March, June, November 2006,
366 June 2008, and February 2009 (Pearson and Spearman's R coefficients >0.98, Fig. 2). The co-
367 variation slope in March (6.44±0.18, Table 3) fully agrees with that observed in January
368 (6.17±0.25), and a set of slopes lower than 6 (Table 3) is observed for June 2006 (5.30±0.19),
369 November 2006 (4.80±0.43), June 2008 (5.11±0.30) and February 2009 (5.16±0.32), though
370 generally higher than that caused by evaporation (4.19±0.09, Fig. 2). Groundwater in the
371 watershed is extensively used for irrigation, which implies irrigation-return flow (Dewandel et
372 al., 2007a) that may be affected by evaporation. Intensive pumping may result in mixing
373 between enriched irrigation-return-flow water and more depleted groundwater (Basu et al.,
374 2002; Zheng et al., 2005).
375 The rural socio-economy in the Maheshwaram watershed is based on traditional
376 agriculture, the main crop being rice that requires much irrigation water. In semi-arid climates
377 (Simpson et al., 1992), a major part of the water used for rice production returns to the
378 atmosphere through the combined effects of evaporation and transpiration. Both processes
379 cause enrichment of the residual water in heavier isotopes, evaporation leading to stronger

enrichment than transpiration (Clark and Fritz, 1997). Simpson et al. (1992), studying the flooding of rice paddies in Australia, found a slope of the δ^2H–$\delta^{18}O$ relationship for the return-flow water similar to that observed in evaporation pans in the same region. Therefore, evaporation would cause a shift for the slope of the δ^2H–$\delta^{18}O$ co-variation in groundwater towards the lower value by the end of the irrigation period in June and May, which would remain low up to the end of the recharge period (after the end of the monsoon in November, plus the transfer through the unsaturated zone). Maréchal et al. (2006) calculated that around 40% of the pumped water returns to the aquifer, and Dewandel et al. (2007a) showed the irrigation-return-flow coefficients (ratio between pumping abstraction versus return flow) to be 10% for flowers, 25% for vegetables and around 50% for rice. This means that the effect of the return flow on the δ^2H–$\delta^{18}O$ signature of groundwater is variable as a function of land use. Taken as a whole over the watershed, the observed small effect on δ^2H and $\delta^{18}O$ in groundwater, which show about the same values as those observed in January during the collection period (Table 3), suggests that the return-flow process has a relatively minor impact on the δ^2H–$\delta^{18}O$ signature of groundwater even if it is important (around 80% of the aquifer volume on a yearly basis, Dewandel et al., 2006). This will be further discussed hereafter when comparing the data at the open-end well scale, as a working hypothesis could be the scale effect because land-use patterns differ in the watershed (de Condappa, 2005), with paddy fields dominating in some parts compared to grape and fruit growing in others.

5.2.2 Downscaling water dynamics: land-use effect at the bore-well scale

There is some variation in the stable-isotope composition between sites, suggesting a heterogeneous origin of the water in the aquifer; this first heterogeneity is related to the variation in recharge as demonstrated before. Investigation of the water dynamics should consider specific use of a well, for which several features can be stated. First, there is a

405 variation or lack of variation in site(s) that may reflect different processes. Hereafter, we
406 consider the case of open-end wells located in parts of the watershed with different water use.
407 First we will investigate the effect of moderate use of groundwater for cultivation from three
408 open-end wells. The first is the little-used open-end well M57 that supplies a dress factory,
409 the two others are open-end wells M12 and M14, respectively used for drip irrigation of grape
410 vines and mango trees. After that, we consider the larger use of groundwater from open-end
411 wells M30, 35, 50 and 53, used for rice growing and vegetable- and flower cultivation.

412 Records for January, March, June and November 2006 were collected for open-end
413 wells M12, 14 and 57 (Fig. 5) plus June 2008 and February 2009 for M12 and M57. For
414 open-end well M14 there is no variation between the periods, and the data plot close to the
415 meteoric water lines and the mean weighted monsoon value of 2006. This suggests that
416 recharge is rapid and concerns the two monsoon periods, as the January values for $\delta^{18}O$ and
417 $\delta^{2}H$ reflecting recharge (Fig. 2) fall on the meteoric water lines. The groundwater is not
418 affected by evaporation and the $\delta^{18}O$ and $\delta^{2}H$ values of the groundwater mimic those of the
419 mean weighted monsoon, suggesting that recharge occurs during the monsoon period from
420 June to December, with physical parameters of soil and saprolite that allow fast and direct
421 recharge (Mathieu and Bariac, 1996). It is obvious that evaporation, either from percolation
422 through soil and saprolite, or directly from the water table, is nil (Maréchal et al., 2006) as
423 the $\delta^{2}H$–$\delta^{18}O$ values in the aquifer agree with the meteoric water input. Following the
424 recharge period, the other surveys show similar $\delta^{18}O$ and $\delta^{2}H$ values, suggesting that the
425 water body supplying the water in open-end well M14 is the same throughout the period,
426 leading to the conclusion that no return flow occurs during drip irrigation of mango trees.

427 Open-end well M57 functioned similarly to open-end well M12 for the first five
428 periods, without variation in the $\delta^{2}H$–$\delta^{18}O$ values between the first four periods whose data
429 plot close to the meteoric water lines and the mean weighted monsoon value of 2006. This

agrees with recharge during the June to December monsoon period, with soil and saprolite characteristics that allow fast and direct recharge to be dominant. The groundwater around open-end well M57 supplies a dress factory and a recent increase in the pumping frequency has shown a shift of the last collected sample (February 2009) along the evaporation line. The response of the aquifer to this change in water abstraction is relatively rapid as the time interval is around 8 months (between June 2008 and February 2009).

Open-end well M12 functions differently. Even though the three periods of January, March and June 2006 had similar $\delta^{18}O$ and $\delta^{2}H$ values, they all plot along the evaporation line. For November 2006, after the recharge period, the groundwater values are close to those of the mean monsoon, again suggesting rapid recharge (Mathieu and Bariac, 1996) without any impact from evaporation. In June 2008, the value was close to that of November 2006, but plotted differently to those observed in June 2006 and February 2009, plotting close to November 2006 and June 2008 values but different from the March 2006 one. This suggests that recharge was sufficiently minor to balance the enriched $\delta^{18}O$ and $\delta^{2}H$ values observed between January and June 2006, but was strong enough to affect the groundwater $\delta^{18}O$ and $\delta^{2}H$ values between November and February 2009. But, as the $\delta^{18}O$ and $\delta^{2}H$ values in groundwater differ from the meteoric water lines through evaporation during the period between January and June 2006, this may indicate that the water body from which the water is pumped was affected by returned irrigation flow. On the other hand, the water body seems to be less affected by evaporation during the period from November 2008 to February 2009, suggesting less water use in this area where grape vines are drip irrigated. A rice paddy is located close to the open-end well, affecting the groundwater body during the rice-growing season (not all the time) through a partly identified return irrigation flow.

We now consider open-end wells M30, 35, 50 and 53, used for rice growing and vegetable- and flower cultivation. Data for all five periods were collected for open-end wells

455 M50, 53 and 30, and for four periods for open-end well M35 (Fig. 5, cont'd). All wells are
456 located near paddy fields and used throughout the irrigation period for flooding the paddies
457 twice a day, all points evolving along the evaporation line. This agrees with groundwater
458 pumping during the irrigation period from the same water body, any compositional change
459 being only controlled by returned irrigation flow. The January values for the open-end wells
460 reveal that all were affected by evaporation as the values depart from the meteoric water lines,
461 but all are also different from the mean weighted 2006 monsoon value, suggesting once again
462 that fast and direct recharge is dominant. Moreover, they evolve similarly during the irrigation
463 period. The groundwater from well M53 falls on the evaporation line, with the March and
464 June 2006 points being close to that of the January recharge, indicating abstraction from the
465 same water body during the irrigation period. The points collected in November 2006 and
466 February 2009 show a slightly more evaporated signature, probably reflecting a returned
467 irrigation flow rather than a change in the water origin, which was also observed in June
468 2008. The groundwater from well M50 evolved similarly from recharge in January plotting
469 along the evaporation line up to March, and June samples that migrated along the evaporation
470 line. One key observation concerns the location along the evaporation line of the February
471 2009 samples that plot with the most strongly shifted values, indicating that either the return
472 flow was large at that time, or that the monsoon recharge was not yet visible in the $\delta^{18}O$ and
473 $\delta^{2}H$ signatures of the groundwater. For well M35 the January and March samples do not
474 differ in signature, but evaporation strongly affected the June ones resulting in a heavy-
475 isotope enrichment of the water. Such evidence of evaporation is not linked to processes
476 affecting the water table and the only way to explain such evaporation is by large returned
477 irrigation flow after enrichment of the water through evaporation in the paddy fields and
478 transpiration from the rice (Simpson et al., 1992). The June samples for both 2006 and 2008
479 thus represent a clear mixture of the groundwater that was used for irrigation between January

480 and March with the strongly evaporated returned irrigation flow. The November sample lies
481 on the same evaporation line as the other samples of the same well, but with $\delta^{18}O$ and $\delta^{2}H$
482 values between those of June and March, showing a shift back to the monsoon value along the
483 LMWL corresponding to the end of the 2007 monsoon. This implies that the groundwater
484 collected in November was partly controlled by the signature of the (mostly evaporated)
485 return flow and by the recharge signature of the SW Monsoon. For February 2009, similar to
486 well M50, $\delta^{18}O$ and $\delta^{2}H$ plot with the most shifted values, again indicating that the
487 groundwater is largely controlled by the signature of the evaporated return flow. Considering
488 that the February sample still includes part of the 2008 monsoon, the $\delta^{18}O$ and $\delta^{2}H$ values
489 indicate a shift back to the monsoon value and thus that the maximum of the $\delta^{18}O$ and $\delta^{2}H$
490 signatures of the groundwater affected by return flow may be higher.

491 In case of such binary mixing, the following equation applies:

492 $$M = a\,EM_1 + (1- a)\,EM_2 \qquad \text{(eq. 1)}$$

493 where M corresponds to the mixture, EM_1 and EM_2 to the two end-members, and a being the
494 mixing parameter, i.e. the proportion of EM1 and EM2 in the mixing. This gives for a

495 $$a = (M-EM_2)/(EM_1-EM_2) \qquad \text{(eq. 2)}$$

496 Considering the November sample as the mixture in M50, the June samples as EM_1
497 and the January one as EM_2, mixing parameter a can be calculated by using equation 2. The
498 result shows that around 70% ± 0.5 (propagated error according to classical formulae of
499 equations 2 derivatives) of the water in the November sample comes from EM_1 (June
500 samples) and around 30 % ± 0.1 (propagated error) from EM_2 (January recharge). Parameter
501 a suggests that most of the recharge through soil and the unsaturated zone occurs between
502 November and January. For the M35 case, we can also consider the November sample as the
503 mixture and the January sample as the recharge (EM_2), defining the returned flow as the most
504 shifted value with $\delta^{18}O$ around 0.5‰. Using equation 2, mixing parameter a gives around

505 50% for each end-member, showing that groundwater like that of November can be affected
506 for around 65% ± 3 (propagated error) by return flow, agreeing with the estimate given by
507 Dewandel et al. (2007a) for the irrigation return-flow coefficients of around 50% for rice.

508 Open-end well M30 is characterized by a more marked NE-monsoon recharge with
509 values close to the mean weighted monsoon value. It experienced evaporation as the recharge
510 values (January sample) depart from the meteoric water lines and the March and June 2006
511 samples plot along an evaporation line, both values being similar but with a more marked
512 evaporation signal compared to the January sample. The June and November 2008 and
513 February 2009 δ^2H and $\delta^{18}O$ values are increasingly marked by the evaporation signal, though
514 with a less evaporated signal than that found in well M35. The influence of returned flow is
515 strongly suggested. Considering the November sample as the mixture, the February samples
516 as EM_1 and the January one as EM_2, mixing parameter a can be calculated with equation 2
517 showing that around 80% ± 12 (propagated error) of the water in the November sample comes
518 from EM_1 (February sample) and around 20% ± 4 (propagated error) from EM_2 (January
519 recharge). Here, parameter a suggests that groundwater like the November one can be
520 affected around 80 ± 12 % by return flow, a higher value than the 50% estimate of Dewandel
521 et al. (2007a) on the irrigation return-flow coefficients for rice.

522 The M35 and M30 calculations led to the conclusion that isotopes of the water
523 molecule, at the bore-well scale, may help in quantifying the land-use effect, i.e. return flow.

524

525 *5.2.3 Effect of land use: impact on salinity and stable-isotope signature of the groundwater*

526
527 In order to evaluate the source of salt in groundwater at the watershed scale, chloride
528 concentrations were plotted against the $\delta^{18}O$ signature of the groundwater (Fig. 6). As the
529 bedrock contains no evaporites, chloride concentrations in groundwater do not derive from
530 weathering and must originate from both evaporation of rainwater and human activity

(Négrel, 1999; 2006). Data were plotted with those from Sukhija et al. (2006), obtained in weathered/fractured granite near Hyderabad (India), 30 km north of Maheshwaram. The highest Cl^- concentration in rainwater, $(Cl)_{ref}$, was determined according to the method defined by Négrel et al. (1993); it was calculated with the chloride content in rainwater, a mean weighted value of close to 1.9 mg L^{-1} during the monsoon, multiplied by the concentration factor F (Négrel, 1999). This factor F represents the concentration effect of evapotranspiration and is related to the total quantity of rainwater P (in mm) and the evapotranspiration process E (in mm) by the equation F = P/(P-E). According to the data given by Maréchal et al. (2006) for the watershed, F ranges between 4.5 and 11, leading to a maximum of rain-derived Cl of 8 to 20 mg L^{-1}. The lowest chloride concentrations observed in Maheshwaram groundwater are <5 mg L^{-1} (Pauwels et al., 2007) and thus only some samples can be considered as representative of the natural background by rain input without human influence. However, the samples with the highest chloride concentrations are also those with the highest nitrate concentrations, suggesting a common origin for these two elements (domestic sewage, *in-situ* sanitation, livestock farming, fertilizer spreading). Some groundwater with a $\delta^{18}O$ signature similar to that of the mean monsoon rain input, i.e. around -3.5 to -4‰, shows a large variation in Cl content (Fig. 6), from less than Cl_{ref} with a minimum of 2.6 mg L^{-1} up to 250 mg L^{-1}, whereas with a more enriched $\delta^{18}O$ signature of around -3‰ the Cl content is >400 mg L^{-1}. This could be due to several steps of evaporation year after year. However, if mixing occurs, due to groundwater exploitation for example, a poor correlation might be observed (Kattan, 2008).

On Figure 6, according to the pan-evaporation experiment, the line where groundwater variations are due only to recharge (i.e. monsoon input, Fig. 3a, b) and evaporation (percolation through soil and saprolite), should show a weak impact on the $\delta^{18}O$ and Cl^- contents, as it starts from the mean rain input but never reaches the maximum of rain-derived

556 Cl^- of up to 20 mg L^{-1}. Thus, considering one-step evaporation processes, the Cl^- content
557 should only reach a low value, around 5 mg. L^{-1}.

558 In order better to understand the joint evolution of Cl^- and $\delta^{18}O$, we created a daily
559 mass-balance model covering the 20-year period of overpumping of the Maheshwaram
560 watershed, which started close to the beginning of the Green Revolution. Overexploitation
561 can be seen in the strongly declining water table caused by a negative groundwater balance
562 (Maréchal et al., 2006). Starting with about 10 open-end wells in 1985, the watershed
563 contained more than 150 open-end wells in 1995 and up to 700 in 2005. For Cl, rainfall is the
564 only source to be considered in the model as man-induced Cl inputs do not influence the O-
565 isotopes. Furthermore, no Cl sink is considered as overpumping of the groundwater leads to
566 endorheic functioning of the watershed (Maréchal et al., 2006) and groundwater becomes
567 increasingly salty though without reaching oversaturation with respect to Cl-solid phases
568 (Pauwels et al., 2007). Soils in the watershed cannot act as Cl sinks as they are clayey/sandy
569 without an organic layer (de Condappa, 2005).

570 The model considers a constant mean value for rainfall and an identical recharge every
571 year. For rainfall values, we used the mean weighted value of Cl during the monsoon period
572 (1.9 mg L^{-1}), and a mean weighted $\delta^{18}O$ value was used for the June-August period and
573 another for September-November, representing the dual monsoon (Deshpande et al., 2003).

574 The volumes of recharge, pumping and return flow for the simulation are from
575 Dewandel et al. (2007). Even if the volume of water in the aquifer varies within a year, it
576 returns to the same initial value by the end of every year. The initial condition was estimated
577 and concerns the mean piezometric elevation of the water table (617 m on average according
578 our field data over 2002, 2003, 2004; see also Maréchal et al., 2006), the mean bedrock
579 elevation (604 m), and a specific yield of 0.014 (Dewandel et al., 2006, 2007a). The aquifer
580 volume can be calculated and thus for one aquifer volume the rainfall volume (recharge) is

0.5, the volume of the aquifer pumped is 0.96 and the return flow is 0.48 of the pumped volume. Recharge occurs in this model over 120 days. One should also consider the twice yearly rice harvest (Dewandel et al., 2007a). The first rainy season between June and October, Kharif, has an average duration of 137 days when watering is from rainfall and irrigation, the second period between November and April, Rabi, covering 166 days when watering is from irrigation only (Perrin et al., 2006). We also considered a watering period of one month before planting when the pumped volume is 0.1 the normal aquifer volume (Dewandel et al., 2007a).

The isotopic signature of the aquifer $\delta^{18}O_T$ can be calculated as follows:

$$\delta^{18}O_T = \delta^{18}O_{j-1} \times V_{j-1}/V_T + \delta^{18}O_{RF} \times V_{RF}/V_T - \delta^{18}O_p \times V_p/V_T + \delta^{18}O_{Rd} \times V_{Rd}/V_T \quad \text{(Eq. 3)}$$

where:

- $\delta^{18}O_{RF}$ is the isotopic signature of the return flow corresponding to $\delta^{18}O_p$ + a ($\delta^{18}O_p$ being the isotopic signature of the pumped water, and a the daily enrichment in heavy isotopes, assumed from an evaporation pan with a value of 0.35);
- $\delta^{18}O_{Rd}$ is the isotopic signature of rainfall, for which two $\delta^{18}O$ values were used (-1.61‰ for June-August and -6.43 ‰ for September-November);
- V_{RF} is the volume of return flow, daily calculated with the equation $V_{RF} = 0.48 \times V_P$;
- V_P is the pumped volume, daily calculated according to $V_P = 0.96 \times V_{T-1}$/days of pumping (166 for the Kharif period and 137 for the Rabi period);
- V_{Rd} is the volume of direct recharge, daily calculated according to $V_{Rd} = 0.5 \times V_P/ 120$;
- V_T if the total volume according to $V_T = V_{T-1} + V_{RF70} + V_{Rd70} - V_P$ (the volume of return flow and direct recharge are considered over 70 days after the beginning of pumping and rainfall, and V_{T-1} is the aquifer volume the day before).

A similar equation was used for simulating the Cl-content variations:

$$Cl_T = Cl_{j-1} \times V_{j-1}/V_T + Cl_{RF} \times V_{RF}/V_T - Cl_p \times V_p/V_T + Cl_{Rd} \times V_{Rd}/V_T \quad \text{(Eq. 4)}$$

606 The results of the simulation are presented in Figure 7, the annual changes covering 10, 15
607 and 20 years. This allows evaluating both intra-annual and inter-annual variations. From these
608 changes, we can state, first, that the chloride content in the groundwater increases as a time
609 function over 10 to 20 years of aquifer exploitation, while, second, the $\delta^{18}O$ signature does
610 not follow the same evolution and stays within the same range of -3 to -3.5‰ over 10 to 20
611 years of aquifer exploitation. Propagated errors on the $\delta^{18}O$, according to classical formulae of
612 equations 3 derivative agree with the stability of the signal as the values of the error never
613 exceed 0.4‰. After 15 years of aquifer overpumping, the simulation results match some of
614 the observed chloride contents (e.g. around 26 mg L^{-1}) for the groundwater as do the 20-year
615 simulation results with a chloride content of around 34 mg L^{-1}. It is worth noting that the
616 propagated errors on the Cl content, calculated similarly to that of eq.3, never exceed 1 mg L^{-1}
617 and thus the increase of the Cl content as given by the model is not impacted by the
618 uncertainties on the calculation. The simulation after the maximum of groundwater
619 exploitation of 20 years thus yields a Cl content of up to 34 mg L^{-1}, including recharge,
620 evaporation, pumping and return flow, but the maximum chloride content does not correspond
621 to the highest $\delta^{18}O$ signature as illustrated on Figure 8 for the 10^{th} year of aquifer exploitation.
622 The chloride content mainly follows the aquifer-volume fluctuation, whereas the $\delta^{18}O$
623 variations are due to the effects of three processes, i.e. pumping, evaporation and return flow,
624 during the Rabi season. However, the increase of the $\delta^{18}O$ value in the simulation is larger
625 with the direct recharge from the first monsoon. The second monsoon has an opposite effect,
626 the isotopic groundwater signature being more negative. Nevertheless, even if the $\delta^{18}O$
627 signature is marked by the monsoon, the simulation again leads to the conclusion that
628 evaporation causes enrichment in heavy isotopes. The mean $\delta^{18}O$ and $\delta^{2}H$ signatures are
629 higher for the rice-paddy areas than for the other parts of the watershed, clearly showing that
630 land-use (paddy fields, grapes, fruit, etc.), and management of the groundwater resource

631 directly affect the hydrochemistry and isotope signatures ($\delta^{18}O$, $\delta^{2}H$) of the groundwater,
632 notwithstanding the effect of additional anthropogenic inputs, like fertilizer applications, on
633 the hydrochemistry.

634 The high Cl^- contents of <430 mg. L^{-1} (sample M20, Jan. 2006) and 370 mg. L^{-1}
635 (sample M15, Nov. 2006) show a slight deviation from the mean weighted monsoon value in
636 terms of $\delta^{18}O$, suggesting a very small impact of the evaporation process and a large
637 anthropogenic influence that may arise from different sources but cannot be simulated by the
638 model (Figs. 6 and 7). In terms of input, Cl^- and NO_3^- reach very high contents of around
639 940 mg. L^{-1} for Cl (Pauwels et al., 2007) as shown on Figure 6. The data from Sukhija et al.
640 (2006) show a similar relationship, with most "modern" water being Cl^- enriched, owing to
641 the fact that one sample of "old" (a few hundreds to thousands of years old) water had a high
642 Cl^- content without any divergence of the $\delta^{18}O$ value. When nitrates and chlorides are of
643 organic origin, the chemical composition is marked by a lower NO_3/Cl ratio than when they
644 have a mineral source (fertilizer). This variability of the NO_3/Cl ratio suggests a variety of
645 inputs, which agrees with land use in the basin. Poultry farming and a population of 15,000
646 inhabitants provide organic compounds, whereas mineral fertilizer is used in paddies and
647 vegetable gardens.

648 6. Conclusions

649 Stable-isotope analyses of precipitation and groundwater from a tropical hard-rock aquifer
650 (Maheshwaram watershed, Andhra Pradesh, India) defined a detailed and dynamic picture of
651 groundwater sources and flow paths. This endorheic watershed is representative of South
652 Indian conditions in terms of geology (hard rock), land-use, overpumping of the hard-rock
653 aquifer (over 700 bored open-end wells in use), and its socio-economic context. The stable
654 isotopes revealed the following features.

Precipitation samples from two entire monsoon cycles allowed defining the NE and SW monsoon signals, the latter being enriched in stable isotopes compared to the first. The monsoon samples define a Local Meteoric Water Line (LMWL) that is close to the Global Meteoric Water Line (GMWL), and allow calculating the mean weighted monsoon signal.

Groundwater data collected in January allowed defining the recharge isotopic signature in the watershed that fluctuates between the two monsoons, with a shift from the LMWL due to evaporation during percolation through soil and saprolite. Groundwater from the irrigation period (March and June) plots in the same range as that defined in January, reflecting few changes at the watershed scale.

Using individual open-end wells for investigating the downscaling of water dynamics, shows that, for a moderate groundwater use for fruit- and grape growing and light industry, the data plot either close to the meteoric water lines and the mean weighted monsoon value, or on an evaporation line. The first observation suggests that recharge is rapid as the monsoon signal is not transformed during percolation through soil and saprolite, while the second observation suggests a lower recharge rate.

Open-end wells with a heavier use of groundwater for rice paddies and vegetable- and flower growing show a different functioning. Groundwater generally follows the evaporation line, with or without deviation from the mean weighted monsoon data, and a returned irrigation flow with a more evaporated signature can be identified while a mixing model allows calculating the proportion of returned water in one case.

Future work should consider variations in the hydrogeological system (layered, fractured, etc.) and in groundwater collected from different boreholes at various depths, for designing a 3D-isotopic framework. This would be necessary for identifying possible flowpaths in conjunction with a larger exploitation of the groundwater resource. Such work would also aid in generalizing the use of other isotope tools such as Nd and Sr or Pb, and of

newly developed isotope systematics like Ca or Si, in other catchments that may face similar structural problems of groundwater overexploitation. This is of primary importance as groundwater flow and -storage in hard-rock areas are major issues for researchers and water managers, especially with regard to water quality as well as the definition of resources and aquifers and of long-term sustainability.

Acknowledgments. This study was carried out at the Indo-French Centre for Groundwater Research (BRGM-NGRI). The authors thank the French Ministry of Foreign Affairs and the French Embassy in India for their support. This paper has benefited from the research and technical assistance provided by Mohamed Wajiduddin ("fabuleux Wajid"), S. Roy and F. Jouin, and from the collaboration of C. Flehoc (BRGM Mass-Spectrometer team) who made the stable-isotope analyses. Tom Bullen is warmly thanked for his comments on the first version of this paper. We are grateful to Dr. H.M. Kluijver for proofreading and editing the English text. We thank the anonymous reviewers for providing critical comments that improved this manuscript.

References

Allison, G.B., Barner, C.J., Hughes, M.W., Leaney, F.W.J. 1984. Effect of climate and vegetation on $\delta^{18}O$ and δD profiles in soils. *In*: Proceedings of IAEA Symposium, Vienna 1984, 105-123.

AMC, 2002. Analytical Methods Committee. Technical brief No. 10. "Fitting a linear functional relationship to data with error on both variables" (Royal Society of Chemistry).

Barth, S.R. 2000. Stable isotope geochemistry of sediments-hosted groundwater from a Late-Proterozoic-Early Mesozoic section in Central Europe. Journal of Hydrology 235, 72-87.

Ballukraya, P.N., Sakthivadivel, R. 2002. Over exploitation and artificial recharge of hard rock aquifers of South India: issues and options. IWMI-Tata Water Policy Research program, International Water Management Institute, 1-14, available at http://www.iwmi.org/iwmi-tata.

Basu, A.R., Jacobsen, S.B., Poreda, R.J., Dowling, C.B., Aggarwal, P.K. 2002. Response to Harvey, 2002: groundwater flow in the Ganges delta. Science 296, 1563.

Clark, I., Fritz, P. 1997. Environmental Isotopes in Hydrogeology. Lewis Publishers, Boca Raton, New York, 328p.

Craig, H. 1961, Isotopic variations in meteoric waters. Science, 133, 1702.

de Condappa, D. 2005. Étude de l'écoulement d'eau à travers la Zone Non-Saturée des aquifères de socle à l'échelle spatiale du bassin versant. Application à l'évaluation de la recharge au sein du bassin versant de Maheshwaram, Andhra Pradesh, Inde. PhD thesis, University of Grenoble, 361p.

Deshpande, R.D., Bhattacharya, S.K., Jani, R.A., Gupta, S.K. 2003. Distribution of oxygen and hydrogen isotopes in shallow ground waters from Southern India: influence of a dual monsoon system. Journal of Hydrology 271, 226-239.

De Silva, C.S., Weatherhead, E.K. 1997. Optimising the dimensions of agrowells in hard-rock aquifers in Sri Lanka. Agricultural Water Management 33, 117-126.

Detay, M., Poyet, P., Emsellem, Y. Bernardi, A. Aubrac, G. 1989. Development of the saprolite reservoir and its state of saturation: influence on the hydrodynamic characteristics of drillings in crystalline basement (in French). Compt. Rend. Acad. Sci. Paris II 309, 429-436.

Dewandel, B., Lachassagne, P., Wyns, R., Maréchal, J.C., Krishnamurthy, N.S. 2006. A generalized 3-D geological and hydrogeological conceptual model of granite aquifers controlled by single or multiphase weathering. Journal of Hydrology 330, 260-284.

Dewandel, B., Gandolfi, J.M., de Condappa, D., Ahmed, S. 2007a. An efficient methodology for estimating irrigation return flow coefficients of irrigated crops at watershed and seasonal scale. Hydrological Processes, DOI: 10.1002/hyp.6738.

Dewandel, B., Gandolfi, J.M., Ahmed, S. Subrahmanyam, K. 2007b. A Decision Support Tool for sustainable Groundwater Management in semi-arid hard-rock areas with variable agro-climatic scenarios. Current Sciences 92, 1093-1102.

Fontes, J.Ch. 1980. Environmental isotopes in groundwater hydrology. Handbook of environmental isotopes geochemistry, Fritz P. and Fontes, J.Ch. (eds.), Elsevier, Amsterdam, Oxford, New York, 75-140.

Gat J.R. 2008. The isotopic composition of evaporating waters - review of the historical evolution leading up to the Craig-Gordon model. Isotopes in Environmental and Health Studies 44, 5-9.

Gibson, J.J., Sadek, M.A., Stone, D.J.M., Hughes, C.E., Hankin, S., Cendon, D.I., Hollins, S.E. 2008. Evaporative isotope enrichment as a constraint on reach water balance along a dryland river. Isotopes in Environmental and Health Studies 44, 83-98.

Gupta, C.P., Singh, V.S. 1988. Flow regime associated with partially penetrating large-diameter wells in hard rocks. Journal of Hydrology 103, 209-217.

Gupta, S.K., Deshpande, R.D. 2005. Groundwater isotopic investigations in India: What has been learned? Current Science 89, 825-835.

Gupta, S.K., Deshpande, R.D., Bhattacharya, S.K., Jani, R.A. 2005. Groundwater $\delta^{18}O$ and δD from central Indian Peninsula: influence of the Arabian Sea and the Bay of Bengal branches of the summer monsoon. Journal of Hydrology 303, 38-55.

Jhajharia, D., Shrivastava, S.K., Sarkar, D., Sarkar, S. 2009. Temporal characteristics of pan evaporation trends under the humid conditions of northeast India. Agricultural and Forest Meteorology 149, 763-770.

Kattan, Z. 2008. Estimation of evaporation and irrigation return flow in arid zones using stable isotope ratios and chloride mass-balance analysis: Case of the Euphrates River, Syria. Journal of Arid Environments 72, 730-747.

Kendall, C., McDonnell, J.J. 1998. Isotope Tracers in Watershed Hydrology. Elsevier, 839p.

Kulkarni, K.M., Navada, S.V., Rao, S.M., Nair, A.R., Kulkarni, U.P., Sharma, S. 1995. Effect of the Holocene climate on composition of groundwater in parts of Haryana, India. IAEA-SM-336/36. In Proceedings of the Symposium on isotopes in water resources management, Vienna, March 1995. 439-454.

Kumar, B., Athavale, R.N., Sahay, K.S.N. 1982. Stable isotope geohydrology of the Lower Maner Basin, Andhra Pradesh, India, Journal of Hydrology 59, 315-330.

Kumar, D., Ahmed, S. 2003. Seasonal behaviour of spatial variability of groundwater level in a granitic aquifer in monsoon climate. Current Science 84, 188-196.

Lee, K.S., Kim, J.M., Lee, D.R., Kim, Y., Lee, D. 2007. Analysis of water movement through an unsaturated soil zone in Jeju Island, Korea using stable oxygen and hydrogen isotopes. Journal of Hydrology 345, 199-211.

783 Majumdar, N., Majumdar, R.K., Mukherjee, A.L., Bhattacharya, S.K., Jani, R.A. 2005. Seasonal variations in
784 the isotopes of oxygen and hydrogen in geothermal waters from Bakreswar and Tantloi, Eastern India:
785 implications for groundwater characterization. J. Asian Earth Sci. 25, 269-278.
786
787 Mathieu, R., Bariac, T. 1996. An isotopic study (^{2}H and ^{18}O) of water movements in clayey soils under a
788 semiarid climate. Water Resources Research 32, 779-789.
789
790 Maréchal J.C., Dewandel, B. Subrahmanyam. K. 2004. Contribution of hydraulic tests at different scales to
791 characterize fracture network properties in the weathered-fissured layer of a hard rock aquifers. Water Resources
792 Res., 40, W11508.
793
794 Maréchal, J.C., Dewandel, B., Ahmed, S., Galeazzi, L., Zaidi, F.K. 2006. Combined estimation of specific yield
795 and natural recharge in a semi-arid groundwater basin with irrigated agriculture. Journal of Hydrology 329, 281-
796 293.
797
798 Mukherjee, A., Fryar, A.E., Rowe, H.D. 2007. Regional-scale stable isotopic signatures of recharge and deep
799 groundwater in the arsenic affected areas of West Bengal, India. Journal of Hydrology 334, 151-161.
800
801 Murad A.A., Krishnamurthy R.V. 2008. Factors controlling stable oxygen, hydrogen and carbon isotope ratios in
802 regional groundwater of the United Arab Emirates (UAE). Hydrological Processes 22, 1922-1931.
803
804 Nahon, D.B. 1991. Introduction to the petrology of soils and chemical weathering. J. Wiley & Sons Ed., 313p.
805
806 Nair, A.R., Navada, S.V., Kulkarni, K.M. Kulkarni, U.P., U.P., Joseph, T.B. 1999. Environmental isotopes
807 studies in the arid regions of western Rajasthan, India. TecDoc IAEA 1207, 41-57.
808
809 Navada, S.V., Nair, A.R., Sinha, U.K., Kulkarni, U.P., Joseph, T.B. 1999. Application of isotopes and chemistry
810 in unsaturated zone in arid areas of Rajasthan, India. TecDoc IAEA 1246, 119-130.
811
812 Négrel, Ph., 1999. Geochemical study of a granitic area - The Margeride Mountains, France: chemical element
813 behavior and $^{87}Sr/^{86}Sr$ constraints. Aquatic Geochemistry 5, 125-165.
814
815 Négrel, Ph., Lachassagne, P. 2000. Geochemistry of the Maroni River (French Guyana) during low water stage:
816 Implications for water rock interaction and groundwater characteristics. Journal of Hydrology 237, 212-233.
817
818 Négrel, Ph. 2006. Water-granite interaction: clues from strontium, neodymium and rare earth elements in
819 saprolite, sediments, soils, surface and mineralized waters. Applied Geochemistry 21, 1432-1454.
820
821 Négrel, Ph., Dewandel, B., Gandolfi, J.M., Dayal, A.M., Pauwels, H., Roy, S., Flehoc, C. 2007. Stable isotope
822 hydrogeology of the Maheshwaram watershed (Andra Pradesh, India). 3rd International Groundwater Conference
823 (IGC-2007) on Water, Environment and Agriculture, Feb. 7-10, 2007, Combinatore, India. In Groundwater
824 Resources Assessment, Recharge and Management, Macmillan Advanced Research Series, M.V. Ranghaswami,
825 K. Palanisami, C. Mayilswami eds., 214-221.
826
827 Négrel, Ph., Machard de Gramont, H., Lemière, B., Billaud, P., Sengupta, B. 2007. Hydrogeochemical
828 processes, mixing and isotope tracing in hard rock aquifers and surface waters from the Subarnarekha river
829 basin, (east Singhbhum district, Jharkhand state, India). Hydrogeology Journal 15, 1535-1552.
830
831 Pauwels, H., Roy, S., Négrel, Ph., Ahmed, S., Dewandel, B., Gandolfi, J.M., Atal, S. 2007. Genesis and control
832 of fluoride concentrations in groundwater of a small agricultural watershed (Maheswharam, Andhra Pradesh,
833 India). 3rd International Groundwater Conference (IGC-2007) on Water, Environment and Agriculture, Feb. 7-
834 10, 2007, Combinatore, India. In Groundwater Quality and Environment, Macmillan Advanced Research Series,
835 M.V Ranghaswami, K. Palanisami, C. Mayilswami eds., 158-164.
836
837 Perrin, J., Dewandel, B., Aulong, S., Ahmed, S., Hrkal, Z., Krazny, J., Mascre, C., Massuel, S., Mukherji, A.,
838 Samad, M. 2006. SUSTWATER Project Final Scientific Report. BRGM report RP-56913-FR, 137 p.
839
840 Praamsma, T., Novakowski, K., Kyser, K., Hall, K. 2009. Using stable isotopes and hydraulic head data to
841 investigate groundwater recharge and discharge in a fractured rock aquifer. Journal of Hydrology 366, 35-45.
842

Robins, N.S., Smedley, P.L. 1994. Hydrogeology and hydrogeochemistry of a small hard-rock island — the heavily stressed aquifer of Jersey. Journal of Hydrology 163, 249-269.

Sami, K. 1992. Recharge mechanisms and geochemical processes in a semi-arid sedimentary basin, Eastern Cape, South Africa. Journal of Hydrology 139, 27-48.

Simpson, H.J., Herczeg, A.L., Meyer, W.S. 1992. Stable isotope ratios in irrigation water can estimate rice crop evaporation. Geophysical Research Letters 19, 377-380.

Singhal, D.C., Niwas, S., Singhal, B.B.S. 1988. Integrated approach to aquifer delineation in hard rock terrains-A case study from the Banda District, India. Journal of Hydrology 98, 165-183.

Sukhija, B.S., Reddy, D.V., Nagabhushanam, P. 1998. Isotopic fingerprints of paleoclimates during the last 30,000 years in deep confined groundwaters of Southern India. Quaternary Research 50, 252–260.

Sukhija, B.S., Reddy, D.V., Nagabhushanam, P., Bhattacharya, S.K., Jani, R.A., Kumar, D. 2006. Characterisation of recharge processes and groundwater flow mechanisms in weathered-fractured granites of Hyderabad (India) using isotopes. Hydrogeology Journal 14, 663–674.

Tardy, Y. 1971. Characterization of the principal weathering types by the geochemistry of waters from some European and African crystalline massifs. Chemical Geology 7, 253-271.

Taylor, R., Howard, K. 2000. A tectono-geomorphic model of the hydrogeology of deeply weathered crystalline rock: evidence from Uganda. Hydrogeology Journal. 8, 279-294.

Tirumalesh, K., Shivanna, K., Jalihal, A.A. 2006. Isotope hydrochemical approach to understand fluoride release into groundwaters of Ilkal area, Bagalkot District, Karnataka, India. Hydrogeology Journal 15, 589-598.

Wyns, R., Gourry, J.C., Baltassat, J.M., Lebert, F. 1999. Caractérisation multiparamètres des horizons de subsurface (0-100 m) en contexte de socle altéré, in 2ème Colloque GEOFCAN, edited by I. BRGM, IRD, UPMC, pp. 105-110, Orléans, France.

Zheng, Y., Datta, S., Stute, M., Dhar, R., Hoque, M.A., Rahman, M.W., Ahmed, K.M., Schlosser, P., van Geen, A. 2005. Stable isotopes (^{18}O, ^{2}H) and arsenic distribution in the shallow aquifers in Araihazar, Bangladesh. EOS Transactions American Geophysical Union, 86 (52), Fall Meeting Supplement, Abstract H31B-1305.

Figure and table captions

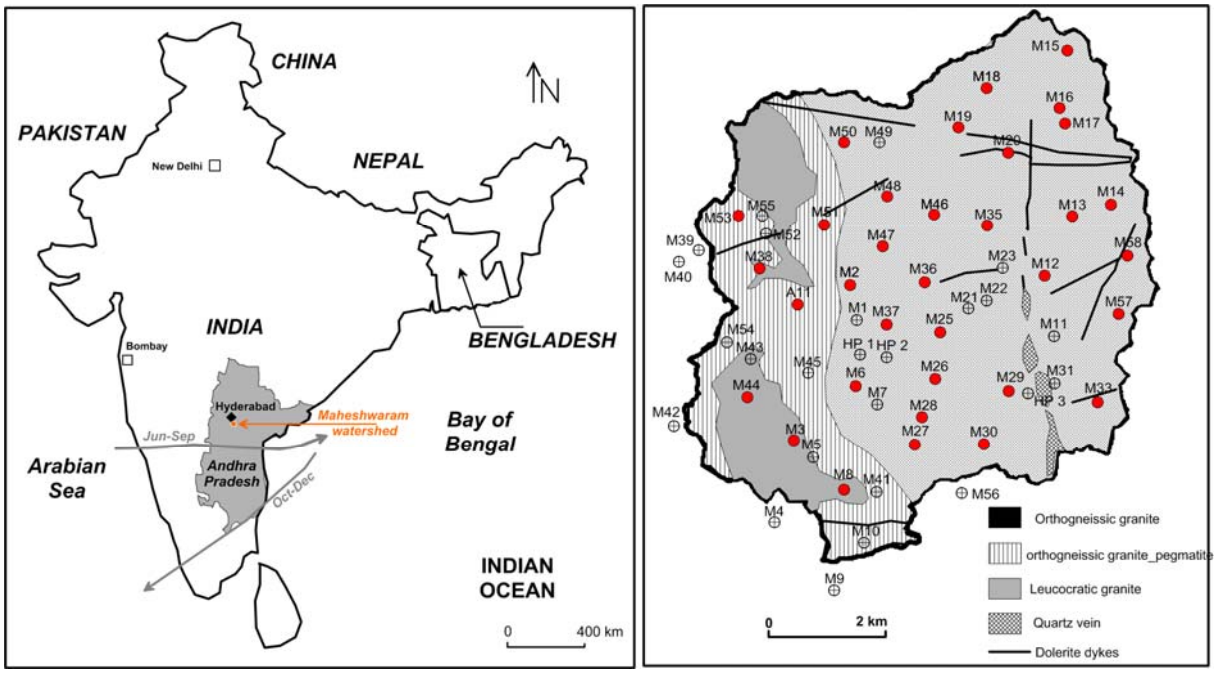

Figure 1. Location of the Maheshwaram watershed (located 35 km south of Hyderabad) in Andhra Pradesh (India), grey arrows indicate the main wind direction (and monsoon origin) for the periods June to September and October to December (Deshpande et al., 2003). Simplified geological map of the Maheshwaram watershed with location of sampled boreholes (Mxx). Black triangle: rain gauge in Maheshwaram village.

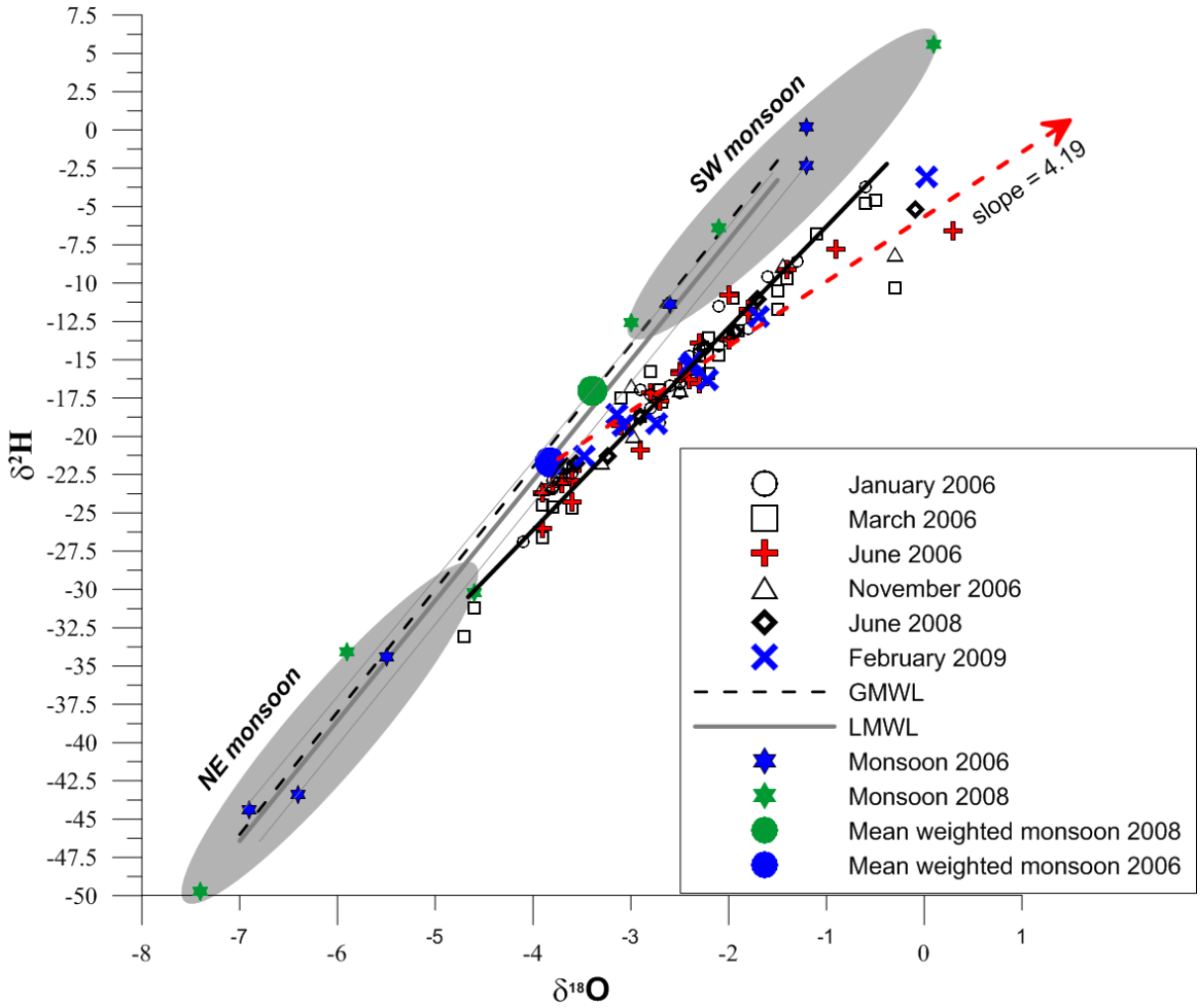

892

893 Figure 2. $\delta^{18}O$-$\delta^{2}H$ plot for groundwater from the Maheshwaram watershed in January (Fig. 2), March, June and
894 November 2006, June 2008 and February 2009. GMWL is the global meteoric water line ($\delta^{2}H = 8\ \delta^{18}O + 10$;
895 Craig, 1961). LMWL is the local meteoric water line defined in this study shown with its 95% uncertainty
896 envelopes. $\delta^{18}O$-$\delta^{2}H$ monsoon samples and weighted means are shown for 2006 and 2008 monsoons. The
897 monsoon data (Kumar et al., 1982) are from the Lower Maner Basin (Andhra Pradesh, north of Maheshwaram).
898 Groundwater in the watershed collected in January 2006 defines a co-variation (black line), the equation is
899 $\delta^{2}H = 6.17\pm0.25 \times \delta^{18}O - 0.54\pm0.67$ (n = 24).

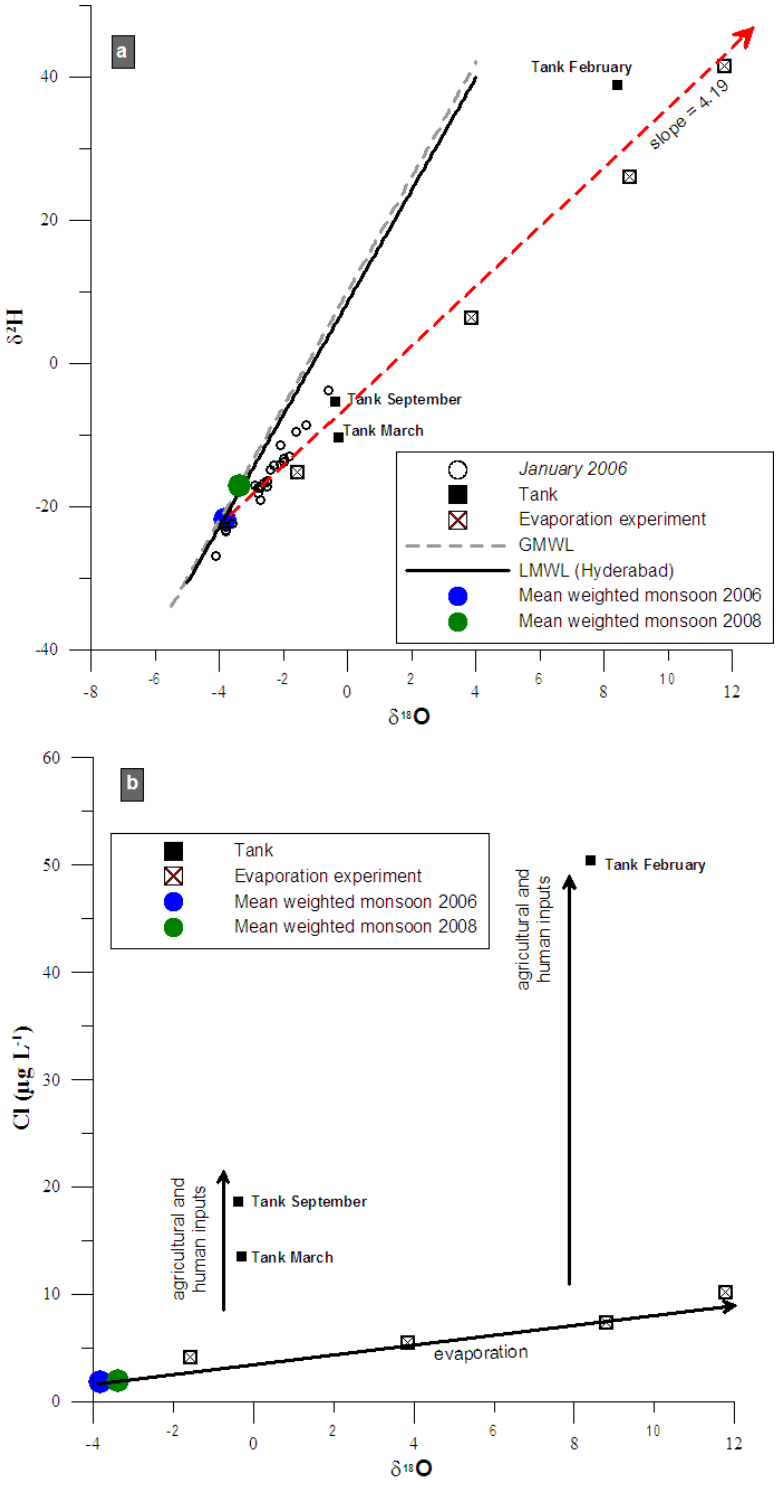

Figure 3. $\delta^{18}O$ - $\delta^{2}H$ plot for groundwater from the Maheshwaram watershed in January (Fig. 4a) and pan-evaporation experiment (Fig. 4b). Tank-sample data are from the only surface water in the watershed. GMWL, LMWL, and monsoon, mean-weighted-monsoon as on Figure 2. $\delta^{18}O$ - Cl content plot of pan-evaporation experiment; mean-weighted-monsoon and tank surface water.

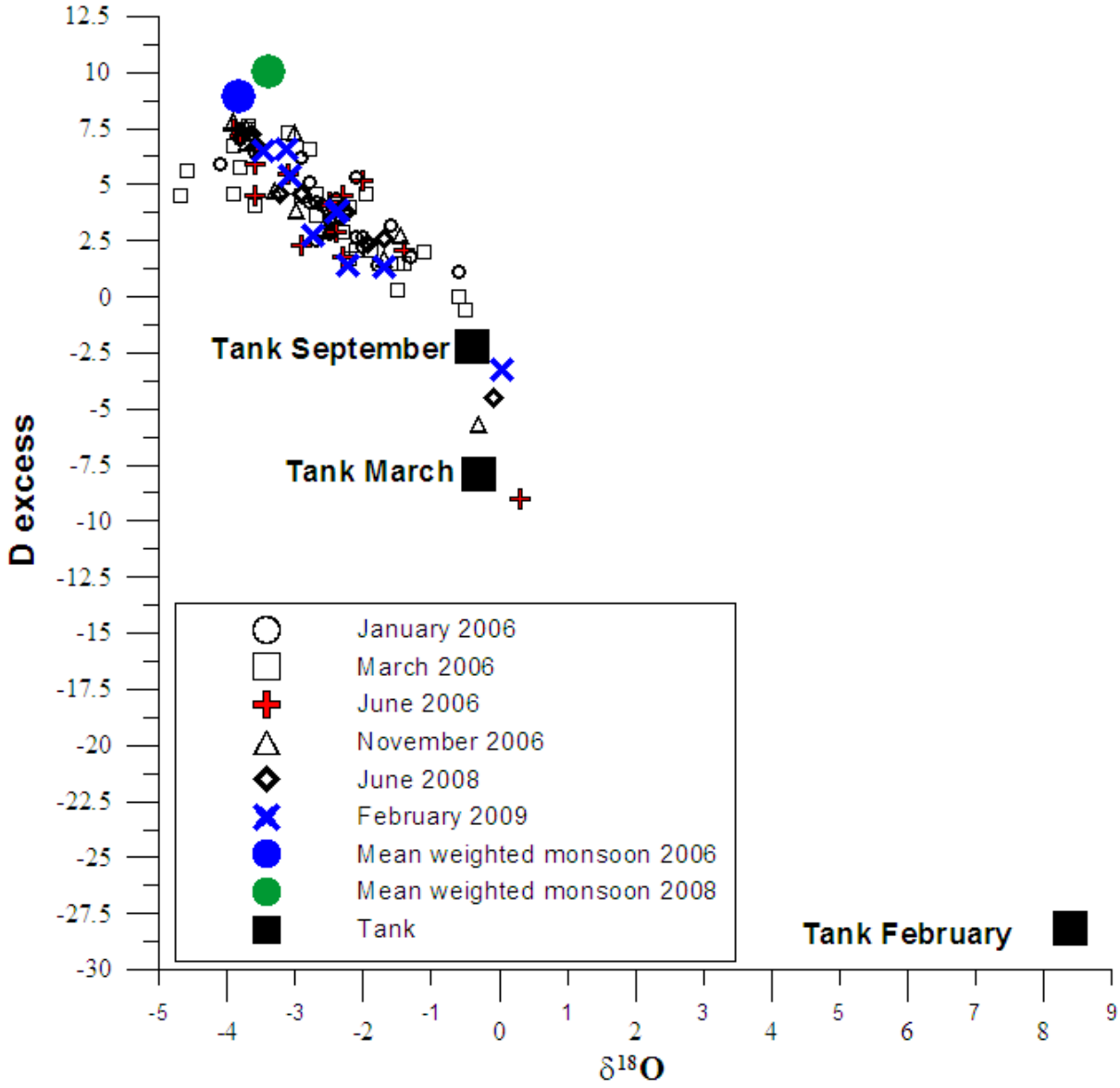

905

906 Figure 4, 'D-excess' *vs.* $\delta^{18}O$ plot for groundwater from the Maheshwaram watershed and for the monsoons (see

907 text).

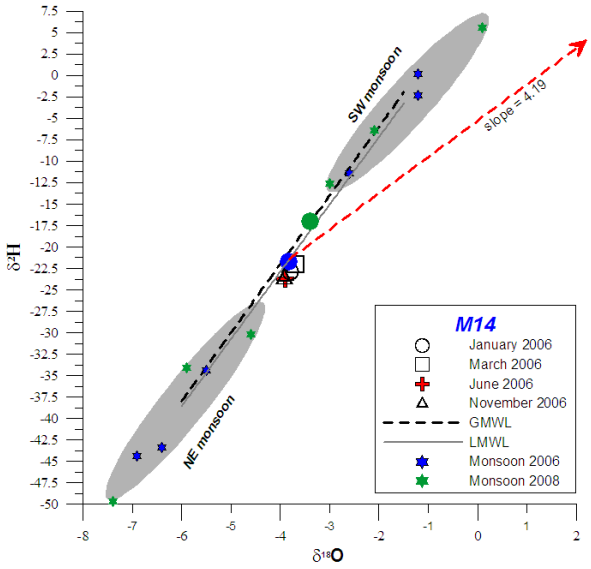
SW monsoon
NE monsoon
slope = 4.19
M14
January 2006
March 2006
June 2006
November 2006
GMWL
LMWL
Monsoon 2006
Monsoon 2008
δ²H
δ¹⁸O

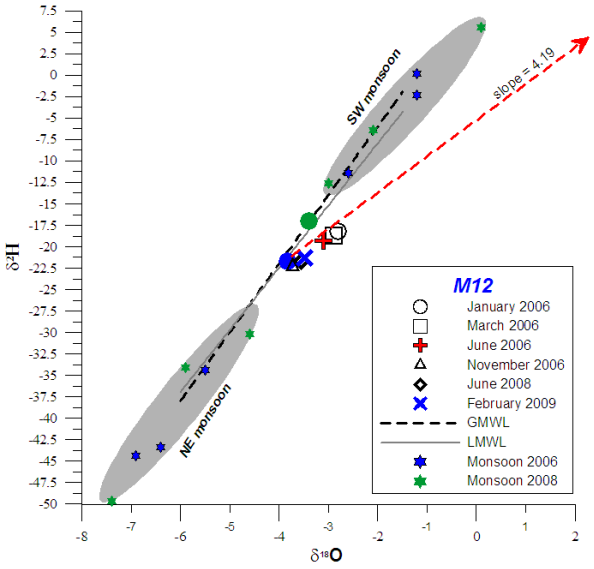
SW monsoon
NE monsoon
slope = 4.19
M12
January 2006
March 2006
June 2006
November 2006
June 2008
February 2009
GMWL
LMWL
Monsoon 2006
Monsoon 2008
δ²H
δ¹⁸O

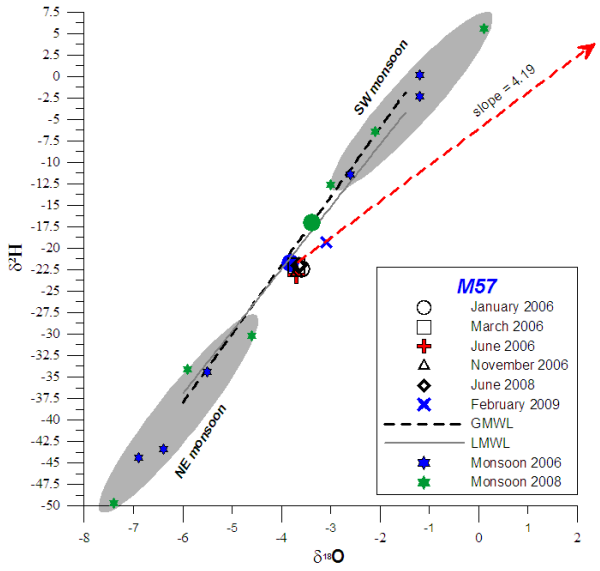
SW monsoon
NE monsoon
slope = 4.19
M57
January 2006
March 2006
June 2006
November 2006
June 2008
February 2009
GMWL
LMWL
Monsoon 2006
Monsoon 2008
δ²H
δ¹⁸O

908

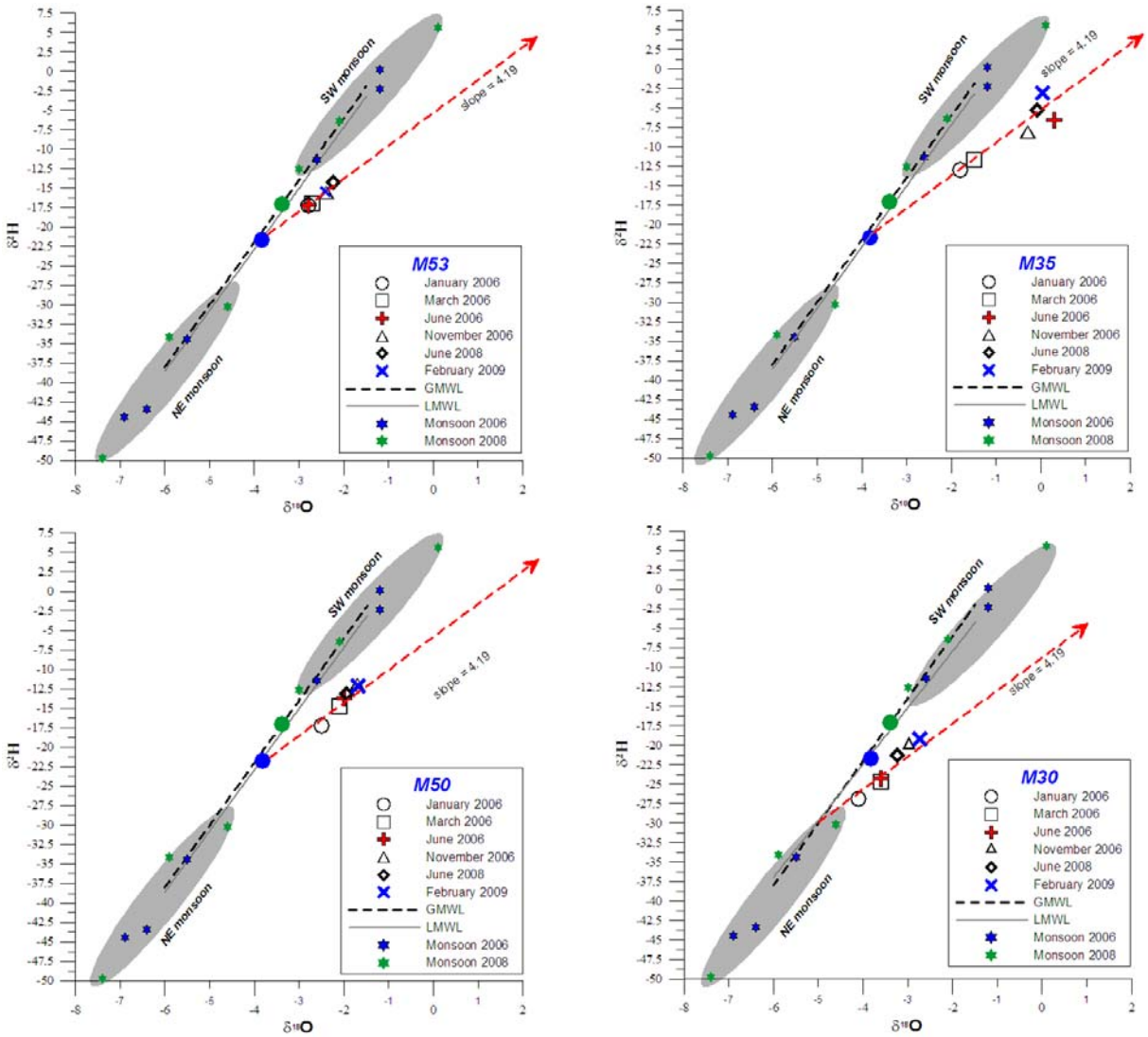

Figure 5a, b. Seasonal $\delta^{18}O$ *vs.* $\delta^{2}H$ variations for selected groundwater collected in the Maheshwaram watershed (moderate use of groundwater for cultivation through open-end wells M12, 14 and 57 and greater use of groundwater through open-end wells M30, 35, 50 and 53; the monsoon, mean-weighted-monsoon, and the slope of the evaporation line are shown as well. As on Figures 2 and 3, GMWL is the global meteoric water line and LMWL is the local meteoric water line.

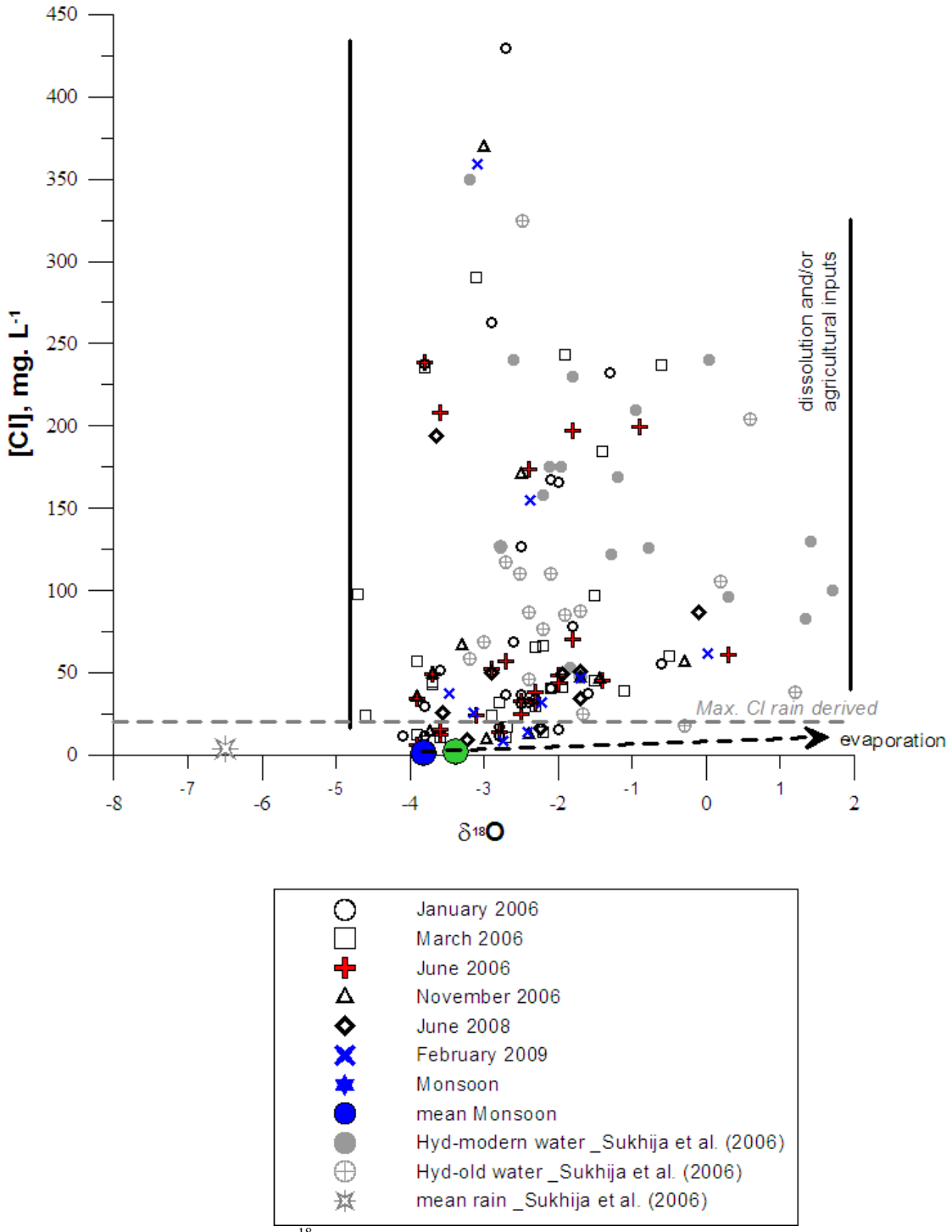

915
916 Figure 6. Cl^- concentration *vs.* $\delta^{18}O$ plot for groundwater from the Maheshwaram watershed, including data for
917 the monsoon, and from the study by Sukhija et al. (2006) in the catchment that comprises Hyderabad and its
918 suburbs. Dashed line corresponds to the one-step evaporation line following the evaporation experiment.

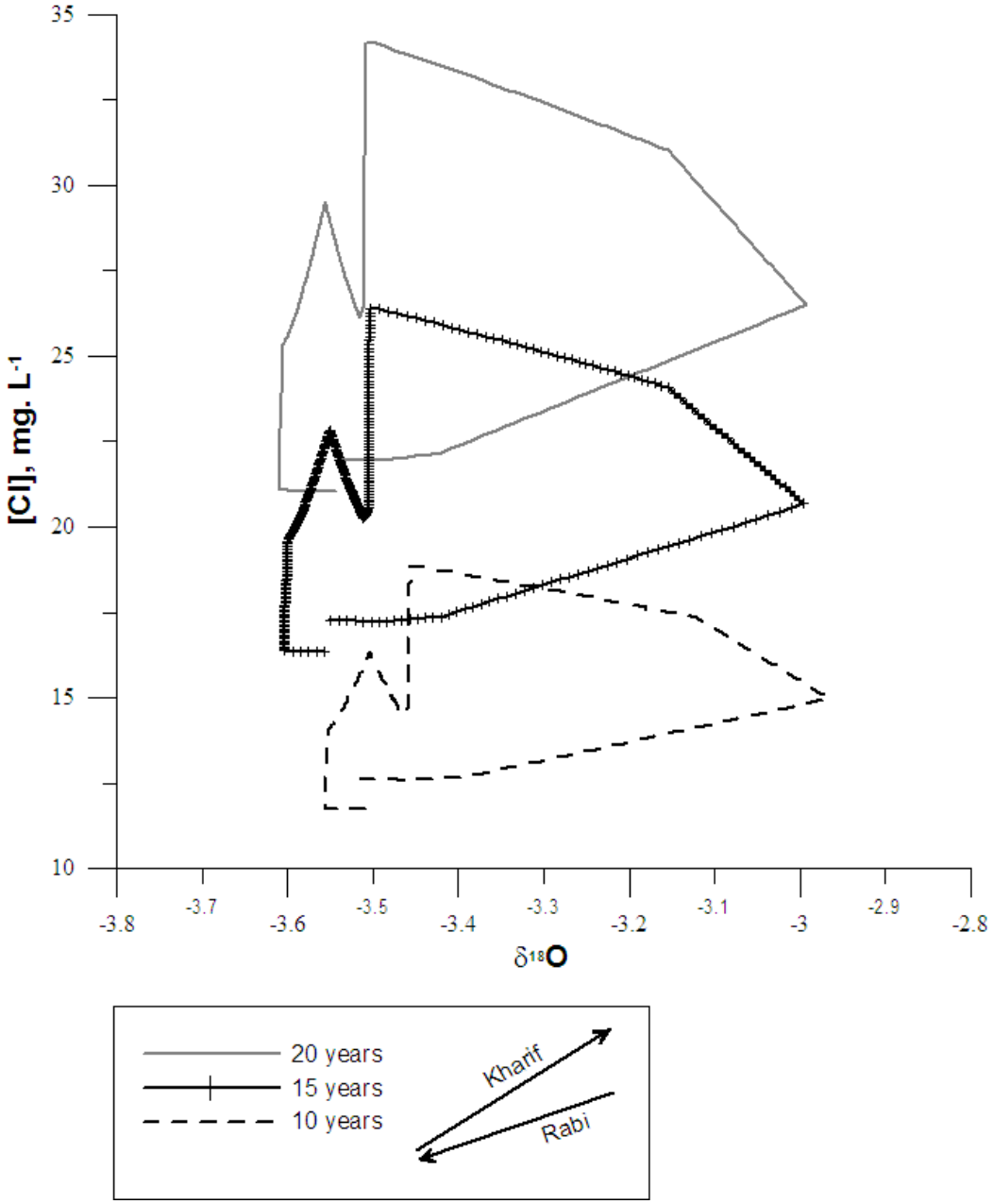

Figure 7. Results of the simulation for Cl- contents and $\delta^{18}O$ signatures over a period of 20 years within the Maheshwaram catchment, considering yearly evolution at 10, 15 and 20 years of overpumping of the aquifer.

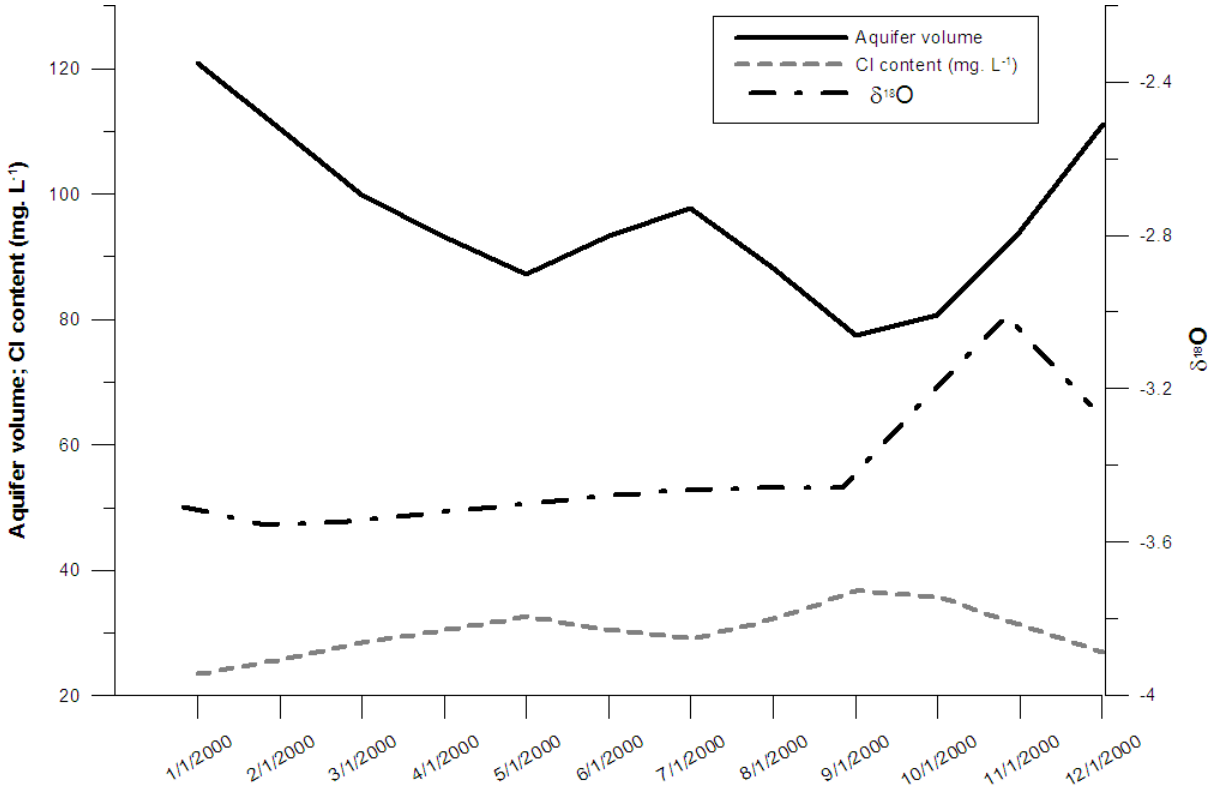

Figure 8. Evolution along the 10th year of overpumping of the Maheshwaram aquifer, for aquifer volume, Cl content, and $\delta^{18}O$.**

Period	δ^2H ‰	$\delta^{18}O$ ‰	Collected volume Rainfall gauge	Collected volume Meteo gauge	Cl^-
	V-SMOW (± 0.8‰)	V-SMOW (± 0.1‰)	L	L	mg. L^{-1}
Monsoon 2006					
June 2006	-2.3	-1.2	0.70	0.60	4.75
July 2006	-11.4	-2.6	1.75	1.50	2.10
August 2006	0.2	-1.2	3.50	2.94	1.53
September 2006	-43.4	-6.4	4.00	4.18	1.30
October 2006	-44.4	-6.9	0.80	0.77	2.55
November 2006	-34.4	-5.5	0.25	0.40	3.30
Mean weighted monsoon 2006	-21.69	-3.83	-	-	1.86
Monsoon 2008					
June 2008	5.6	0.1	0.75	-	nd
July 2008	-6.4	-2.1	2.84	-	nd
August 2008	-12.6	-3	5.30	-	nd
September 2008	-49.7	-7.4	1.45	-	nd
October 2008	-30.2	-4.6	1.25	-	nd
November 2008	-34.1	-5.9	0.40	-	nd
Mean weighted monsoon 2008	-17.05	-3.39	-	-	-

Table 1. Results of stable isotopes of the water molecule ($\delta^{18}O$ and δ^2H), collected volumes, and Cl^- contents for monsoon precipitation collected in Maheshwaram village in 2006.

Sample	T °C	EC µS cm^{-1}	Cl^- mg. L^{-1}	δ^2H ‰ V-SMOW (±0.8‰)	$\delta^{18}O$ ‰ V-SMOW (±0.1‰)	D-excess
January 2006						
A11	27.5	850	34.41	-14.3	-2.3	4.1
M02	28.4	1440	166.22	-13.3	-2.0	2.7
M03	27.2	770	40.64	-11.5	-2.1	5.3
M06	29.8	685	36.98	-19.1	-2.7	2.5
M08	26.6	700	37.58	-9.6	-1.6	3.2
M12	26.0	750	17.34	-18.2	-2.8	4.2
M14	27.6	900	29.75	-22.9	-3.8	7.5
M15	27.9	3310	263.21	-17.0	-2.9	6.2
M16	27.3	1800	238.00	-23.4	-3.8	7.0
M19N	27.4	1470	167.04	-14.1	-2.1	2.7
M20	27.5	3570	429.15	-17.4	-2.7	4.2
M25	28.1	700	31.45	-16.6	-2.5	3.4
M28	26.6	670	15.65	-13.8	-2.0	2.2
M29	25.9	1390	126.84	-16.5	-2.5	3.5
M30	26.3	670	11.70	-26.9	-4.1	5.9
M33	27.7	600	11.78	-23.3	-3.8	7.1
M35N	27.1	1060	77.91	-13.0	-1.8	1.4
M36N	28.8	750	31.86	-14.8	-2.4	4.4
M44	26.7	940	55.77	-3.7	-0.6	1.1
M46	29.3	800	68.91	-16.7	-2.6	4.1
M50	26.9	770	36.82	-17.2	-2.5	2.8
M51	27.3	1830	232.62	-8.6	-1.3	1.8
M53	28.4	810	11.35	-17.3	-2.8	5.1
M57	28.6	1100	51.66	-22.4	-3.6	6.4
March 2006						
A11	27.4	820	29.62	-15.5	-2.3	2.9
M02	28.5	970	97.91	-33.1	-4.7	4.5
M03	26.8	800	41.12	-11.0	-2.0	4.6
M06	28.6	800	45.50	-10.5	-1.5	1.5
M08	27.0	660	38.97	-6.8	-1.1	2.0
M12	26.5	797	24.30	-18.7	-2.9	4.5
M14	27.6	940	42.89	-22.0	-3.7	7.6
M15	28.8	3270	290.07	-17.5	-3.1	7.3
M16	nd	1780	235.28	-24.6	-3.8	5.8
M19N	27.1	180	243.59	-13.1	-1.9	2.1
M20	29.1	1077	57.17	-26.6	-3.9	4.6
M25	29.1	590	17.43	-17.8	-2.7	3.7
M28	27.8	690	13.84	-13.6	-2.2	4.0
M29	26.8	930	66.32	-15.9	-2.2	1.7
M30	27.5	1460	10.81	-24.7	-3.6	4.1
M33	28.2	610	12.18	-24.5	-3.9	6.7
M35N	27.4	1140	96.80	-11.7	-1.5	0.3
M36N	28.6	760	31.96	-15.8	-2.8	6.6
M37	28.6	1490	237.33	-4.8	-0.6	0.0
M44	26.0	940	60.41	-4.6	-0.5	-0.6
M46	28.6	790	65.34	-14.7	-2.3	3.7
M48	27.5	650	24.46	-31.2	-4.6	5.6
M50	27.4	650	40.37	-14.7	-2.1	2.1
M51	27.5	1770	184.74	-9.7	-1.4	1.5
M53	28.0	790	10.72	-17.0	-2.7	4.6
M57	30.1	1080	44.79	-22.1	-3.7	7.5
Tank	nd	nd	nd	-10.3	-0.3	-7.9
June 2006						

A11	28.8	790	31.73	-13.9	-2.3	4.5
M2	nd	nd	173.78	-16.3	-2.4	2.9
M3	28.2	840	48.85	-10.8	-2.0	5.2
M6	27.2	690	38.51	-16.6	-2.3	1.8
M8	nd	nd	45.31	-9.1	-1.4	2.1
M12	nd	nd	24.62	-19.3	-3.1	5.5
M14	28.6	890	34.30	-23.7	-3.9	7.5
M15	28.9	1480	208.46	-22.2	-3.6	6.6
M16	27.8	1740	238.38	-23.2	-3.8	7.2
M25	28.3	650	25.28	-15.8	-2.5	4.2
M29	nd	nd	52.53	-20.9	-2.9	2.3
M30	27.5	720	12.56	-24.3	-3.6	4.5
M33	28.2	640	15.82	-22.9	-3.6	5.9
M35N	nd	nd	60.69	-6.6	0.3	-9.0
M36N	29.0	780	32.59	-15.9	-2.5	4.1
M37	28.7	1160	199.16	-7.8	-0.9	-0.6
M44	nd	nd	70.63	-11.7	-1.8	2.7
M46	28.7	756	57.27	-17.7	-2.7	3.9
M48	nd	nd	6.14	-26.0	-3.9	5.2
M50	nd	nd	43.66	-13.7	-2.0	2.3
M51	27.4	1610	197.50	-12.0	-1.8	2.4
M53	28.9	810	13.90	-17.2	-2.8	5.2
M57	28.8	1060	49.27	-23.1	-3.7	6.5
November 2006						
M2	28.3	1940	170.28	-17.0	-2.5	3.0
M8	nd	Nd	45.74	-8.8	-1.4	2.7
M12	nd	Nd	13.72	-22.3	-3.7	7.5
M14	nd	Nd	34.95	-23.4	-3.9	7.8
M15	28.2	4930	369.61	-16.7	-3.0	7.3
M29	27.5	1350	66.52	-21.7	-3.3	4.7
M30	nd	Nd	9.48	-20.0	-3.0	3.8
M35	nd	1280	56.70	-8.1	-0.3	-5.7
M50	27.4	1300	46.58	-11.9	-1.7	1.7
M53	28.9	1120	12.29	-15.6	-2.4	3.6
M57	nd	nd	49.47	-22.8	-3.7	6.9
June 2008						
M6	27.9	nd	34.10	-11.0	-1.7	2.6
M8	28.7	780	51.15	-11.0	-1.7	2.6
M12	29.2	700	25.73	-21.7	-3.6	6.7
M30	28.3	700	9.66	-21.3	-3.2	4.6
M35	27.7	1200	86.44	-5.2	-0.1	-4.5
M48	28.4	nd	50.41	-18.7	-2.9	4.6
M50	27.7	920	49.10	-13.2	-1.9	2.3
M53	30.1	870	16.55	-14.2	-2.2	3.7
M57	30.6	1510	194.06	-22.0	-3.7	7.2
February 2009						
M2	28.8	1303	154.71	-15.2	-2.4	3.8
M6	27.6	752	31.73	-16.3	-2.2	1.4
M8	23	596	25.88	-18.6	-3.1	6.5
M12	28.6	763	37.30	-21.3	-3.5	6.5
M30	27.7	683	8.40	-19.1	-2.7	2.7
M35	27.5	1085	61.65	-3.0	0.0	-3.3
M50	26.9	982	46.83	-12.2	-1.7	1.3
M53	29.6	857	14.00	-15.4	-2.4	3.8
M57	32	2000	359.01	-19.3	-3.1	5.4
Tank						

Tank March 2006	nd	nd	13.6	-10.3	-0.3	-7.9
Tank November 2006	nd	nd	18.7	-5.4	-0.4	-2.2
Tank February 2009	nd	nd	50.42	38.4	8.4	-28.2

nd = non-determined values

Table 2. Results of field variables (EC in µS/cm; temperature in °C; pH) and stable isotopes of the water molecule ($\delta^{18}O$ and $\delta^{2}H$), in ‰ with reference to V-SMOW (Vienna Standard Mean Ocean Water) for groundwater collected in the Maheshwaram watershed.

Period	Equation	n	R^2
January 2006	$\delta^2H = 6.17 \pm 0.25 \times \delta^{18}O - 0.54 \pm 0.67$	24	> 0.98
March 2006	$\delta^2H = 6.44 \pm 0.18 \times \delta^{18}O - 0.24 \pm 0.50$	26	> 0.98
June 2006	$\delta^2H = 5.30 \pm 0.19 \times \delta^{18}O - 3.33 \pm 0.54$	23	> 0.98
November 2006	$\delta^2H = 4.80 \pm 0.43 \times \delta^{18}O - 4.49 \pm 1.22$	11	> 0.98
June 2008	$\delta^2H = 5.11 \pm 0.30 \times \delta^{18}O - 3.44 \pm 0.77$	9	> 0.98
February 2009	$\delta^2H = 5.16 \pm 0.32 \times \delta^{18}O - 3.51 \pm 0.81$	9	> 0.98

Table 3. Results of $\delta^{18}O$ and δ^2H relationships for the January, March, June and November 2006, June 2008, February 2009 collection periods, n is the number of open end wells collected and R^2 is the correlation coefficient.